NTNU
Norwegian University of Science and Technology
Faculty of Engineering
Department of Mechanical and Industrial Engineering

Vegard Ledal

# Design of Non-conventional Wind Turbine structures with Integrated Design for manufacturing

**NTNU**

Norwegian University of
Science and Technology

Vegard Ledal

# Design of Non-conventional Wind Turbine structures with Integrated Design for manufacturing

Master's thesis in Mechanical Engineering
Supervisor: Geir Ringen
June 2023

Norwegian University of Science and Technology
Faculty of Engineering
Department of Mechanical and Industrial Engineering

**NTNU**
Norwegian University of
Science and Technology

# Preface

This master's thesis is the result of my research project on wind turbines and aluminium, conducted at NTNU. I would like to express my sincere gratitude to my supervisor, Geir Ringen, for his invaluable guidance, feedback, and support throughout the research process.

The purpose of this thesis is twofold. The first task is explore different joining method between the mast and blade of a wind turbine based on functionality, manufacturability and reliability, both made of aluminium. The second task compares different production lines of aluminium, including an integrated production method that collects scrap aluminium and remelts instead of producing primary metal.

The research process involved a comprehensive literature review on wind turbines and aluminium, followed by selecting the joining method through a set-based design methodology that includes dimensioning and confirming the selected method through simulations in Abaqus. The data for the comparison of different production lines of aluminium was collected using various sources such as published literature and secondary sources.

I would like to acknowledge the task given by World Wide Wind, without whom this research would not have been possible. Additionally, I would like to express my appreciation to my family and friends for their unwavering love, encouragement, and support throughout my academic journey.

Vegard Ledal

11/06-2023

# Abstract

The master thesis addresses two key aspects related to offshore wind turbines: joining methods for wind turbine blade and the evaluation of manufacturing value chains. The objective is to explore efficient and sustainable approaches regarding turbine design and production.

Regarding joining methods, two major techniques were examined: standard component that is MIG-welded or using bolt connection, and special purpose extruded T-track with bolt connection. Each method was evaluated based on strength, material use, complexity, and manufacturability. The results indicated that MIG welding offers high strength, low material use, moderate complexity and low manufacturability. Bolt connection provides moderate strength, low material use, low complexity and high manufacturability. The extruded T-track with bolt connection demonstrates high strength, high material use, moderate complexity and moderate manufacturability through simulations in Abaqus.

The assessment of manufacturing value chains focused on three cases: primary aluminium production in China using coal, primary aluminium production in Slovenia using nuclear energy, and gathering post-consumer metal in Norway for remelting. The analysis considered cost and energy emissions for different production volumes. The findings revealed that the integrated production line exhibited high cost and carbon emissions for low production volumes, due to the construction of the factory. For higher production volumes, the values decreased making it the most favorable option. It is important to carefully consider the high investment required in terms of both cost and emissions, as it holds potential benefits for the future.

By considering both joining methods and manufacturing value chains, it becomes possible to design offshore wind turbines that are structurally robust, cost-effective, and environmentally responsible. However, it is important to acknowledge the limitations of the research, including data availability and the need for further collaboration and research to refine the findings.

Overall, this thesis contributes to the knowledge and understanding of joining methods and manufacturing value chains for offshore wind turbines. The insights gained from this research can inform decision-making processes, supporting the development of efficient and sustainable offshore wind turbine designs.

# Sammendrag

Masteroppgaven tar for seg to sentrale aspekter knyttet til offshore vindturbiner: sammenføyningsmetoder for vindturbinblader og evaluering av produksjonsverdikjeder. Målet er å utforske effektive og bærekraftige tilnærminger til turbindesign og produksjon.

Når det gjelder sammenføyningsmetoder, ble to ulike kategorier undersøkt: standardkomponent som er MIG-sveiset eller med boltforbindelse, og spesialekstrudert T-spor med boltforbindelse. Hver metode ble evaluert basert på styrke, materialbruk, kompleksitet og produserbarhet. Resultatene indikerte at MIG-sveising tilbyr høy styrke, lav materialbruk, moderat kompleksitet og lav produksjonsevne. Boltforbindelse gir moderat styrke, lav materialbruk, lav kompleksitet og høy produksjonsevne. Det ekstruderte T-sporet med boltforbindelse demonstrerer høy styrke, høy materialbruk, moderat kompleksitet og moderat produksjonsevne gjennom simuleringer i Abaqus.

Vurderingen av produksjonsverdikjeder fokuserte på tre tilfeller: primæraluminiumproduksjon i Kina ved bruk av kull, primær aluminiumproduksjon i Slovenia ved bruk av kjernekraft, og innsamling av post-consumer metall i Norge for omsmelting. Analysen tok for seg kostnad og energiutslipp for ulike produksjonsvolumer. Funnene avslørte at den integrerte produksjonslinjen viste høye kostnader og karbonutslipp for lave produksjonsvolumer, på grunn av byggingen av fabrikk. For høyere produksjonsvolumer sank verdiene, noe som gjorde det til det mest gunstige alternativet. Det er viktig å nøye vurdere de høye investeringene som kreves både når det gjelder kostnader og utslipp, da det har potensielle fordeler for fremtiden.

Ved å vurdere både sammenføyningsmetoder og produksjonsverdikjeder, blir det mulig å designe vindturbiner til havs som er strukturelt robuste, kostnadseffektive og miljøansvarlige. Det er imidlertid viktig å erkjenne begrensningene ved forskningen, inkludert datatilgjengelighet og behovet for ytterligere samarbeid og forskning for å avgrense funnene.

Samlet sett bidrar denne oppgaven til kunnskap og forståelse av sammenføyningsmetoder og produksjon av verdikjeder for vindturbiner til havs. Innsikten oppnådd fra denne forskningen kan informere beslutningsprosesser, og støtte utviklingen av effektive og bærekraftige offshore vindturbindesign.

# Contents

## List of Figures

## List of Tables

# 1. Introduction

For many years there has been interest in the subject of climate change and global warming. Renewable energy is frequently cited as the most important shift the world can make to fend off the worst consequences of global warming. This is due to the fact that renewable energy sources like solar and wind don't produce greenhouse gases like carbon dioxide, which contributes to global warming. This is referred to when energy is produced, because the equipment to be used must be built and this will obviously lead to emissions. There are a lot more benefits to clean energy than just being green. The expanding industry boosts employment, strengthens the resilience of electric networks, increases access to energy in underdeveloped nations, and lowers energy costs. All of those elements have helped to fuel a resurgence in renewable energy in recent years, with wind and solar power generating more electricity than ever before. More than 7 000 years ago, people first started using the wind as a source of energy. Now, wind turbines that produce power are being installed all over the world [1].

Increasing Europe's offshore wind capacity from 12 GW in 2020 to at least 60 GW by 2030 and 300 GW by 2050 is the aim of the European Commission. It is difficult to decommission offshore projects and reuse/recycle materials like turbine blades, among other things. Research and innovation must incorporate the design for circularity philosophy, and a careful analysis of the materials employed is required [2]. Wind energy is proven to be too valuable a resource to ignore, despite some people's concerns about how wind turbines appear and sound in the distance. Another issue with wind turbines is that they pose a threat to birds and bats, killing hundreds of thousands of them every year. Although this number is not as high as deaths caused by glass collisions or other threats like habitat loss and invasive species, it is still enough for engineers to be working on ways to make wind turbines less dangerous for birds [1].

Offshore wind turbines have a huge potential in using aluminium due to its properties. Aluminium is the third most common element in the crust of the planet, after silicon and oxygen. In other words, there is more aluminium than iron on the globe, and given the amount of aluminium we currently consume, our resources will last us for generations. A piece of aluminium weighs only 2,7 g/$cm^3$, which is only a third of steel. Aluminium is a lightweight and adaptable material that is also an economically sensible choice. Because of its low weight makes it easier to handle in a factory or on a construction site and also results in less energy usage during transportation. Due to its high degree of malleability, aluminium may be formed into a variety of objects, such as computer cases, boat hulls, bicycle frames, and kitchenware. Both in cold and hot temperatures, aluminium is simple to process, and it is possible to make a variety of alloys. Typically, aluminium alloys are utilized to improve the qualities of aluminium for particular engineering constructions and components where lightweight or corrosion resistance are crucial. Magnesium, iron, silicon, manganese, zinc, and copper are the most frequently used elements in aluminium alloys. Thus, aluminium gives complete design flexibility and is appropriate for a variety of functions. Aluminium forms a protective oxide covering that resists corrosion when it reacts with airborne oxygen. Compared to metals like iron or steel, this means fewer maintenance and replacements. Reduced maintenance requirements and fewer replacements are advantageous for the environment and a project's total budget. Few materials can be recycled as effortlessly as aluminium. Recycling primary aluminium only needs about 5% of the energy it took to make it in the first place. In fact, of all the aluminium that has ever been produced, about 75% is still in use [3].

## 1.1. Target

The goal of the master thesis is to create knowledge and understanding about offshore wind turbines and aluminium, and to see if these can be combined. Further, it is desirable to create a connection between the mast and turbine blade based on functionality, manufacturability and reliability. The created model has a safety factor to create a realistic joint, applicable for prototyping. Multiple scenarios and criteria must be considered and a good model platform must be selected and used. These turbines must also be manufactured. Currently, most productions of are separated and carried out in dispersed and global value chain. By having a production-integrated structure, this could happen under the same roof. In order to find any advantages or disadvantages having an production-integrated structure, different cases of aluminium production and shipping will be compared in terms of cost and carbon footprint. The result will hopefully reveal differences, and show which production structure manufacturers should invest in for the future.

## 1.2. Objective

Two different objectives within offshore wind turbines and aluminium will be looked into.

- Explore joining methods with emphasis on manufacturing efficiency and installation among different design alternatives.

- Evaluate different manufacturing value chains for the design alternatives according to cost and energy emission.

## 1.3. Method

Some suitable joining methods for aluminium will be presented, alongside their pros and cons. To determine which joining method is selected and proceeded with on the basis of given criteria, a set-based design approach will be used. Set-based design is a crucial technique or philosophy to improve adaptability and decrease rework. The model is often explained through a funnel like shown in Figure 1. Prior to making important decisions, it is crucial to gather knowledge; set-based design seeks to do just that by breaking the circular dependency. Instead of representing initial needs as point values, the technique represents them as sets or ranges that are later refined during the development effort. Before making important design decisions, such as selecting a concept solution, one should consider trade-offs, design constraints and potential combinations. Therefore, it is favorable to create collections of distinct design options. As the granularity of the solution grows, the sets' sizes eventually decrease. Cross-functional information exchange in parallel subsystem and manufacturing development helps with design decisions [4].
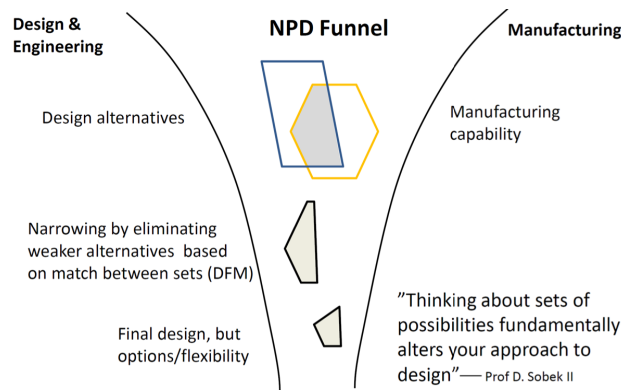


**Figure 1:** Set-based design concept [4]

The selected joining method will be dimensioned to handle the experienced load via an iterative approach. This is a way to continuously refining a concept, design, or product. The process consists of a few simple procedures that you repeat, making adjustments and enhancing your product between each cycle. This process will be continued until the stress result is acceptable [5]. The program that will be used in the iterative process is called Abaqus CAE.

Abaqus/CAE (Complete Abaqus Environment) from Dassault Systèmes, is one of the five essential software packages in Abaqus. Here, one can rapidly and effectively build, update, and visualize sophisticated Abaqus studies with Abaqus/CAE. Modeling, analysis, and result visualization are all integrated within the user-friendly interface. Feature-based, parametric modeling, interactive operation, and scripted operation are just a few of the well-known interactive computer-aided engineering concepts supported by Abaqus/CAE. Users can import CAD models for meshing, import their own geometry, or combine geometry-based meshes without any CAD geometry [6]. The CAD geometry translators make it simple to integrate Abaqus/CAE with other programs by allowing you to import model geometries from CAD systems [7].

The software SOLIDWORKS is one of these CAD-systems. Any business can use SOLIDWORKS' robust yet user-friendly 2D and 3D product development solutions. Leading engineers and designers rely on SOLIDWORKS solutions to develop, collaborate on, and deliver cutting-edge product experiences [8]. The completed model in Abaqus will be exported to SOLIDWORKS through the use of a STEP file. This makes it possible to create mechanical drawings of the finished model which will be attached in the appendix.

Considering the various production lines, obtaining precise values will be challenging due to factors such as negotiated pricing, confidentiality, and proprietary information. Consequently, secondary sources will play a more significant role in acquiring information and estimating values pertaining to the different production lines. The collection of data will be facilitated through digital meetings, email exchanges, and telephone conversations. It is important to approach the results with caution, as they are approximate and based on estimations. Nonetheless, these figures will serve as a foundation for comparison and offer valuable opportunities for further discussion and analysis.

# 2. Wind turbines design and evolution

## 2.1. Evolution of wind turbines

Wind turbines have been in use for a long time. The efficiency, types and area of use have however changed. Back in the day, wind turbines were used to crush grains. Nowadays, wind turbines generate power for thousands of households with two primary classifications of wind turbines. Horizontal-Axis Wind Turbines (HAWTs) and Vertical-Axis Wind Turbines (VAWTs). HAWTs are widely deployed, characterized by their configuration of two or three long, slender blades. These blades are oriented to align with the wind's direction, ensuring optimal performance. Conversely, VAWTs exhibit a distinct design with shorter, broader blades that assume a curved shape [9]. With the change in use and increase in efficiency, the size of the wind turbine has also increased as shown in Figure 2.
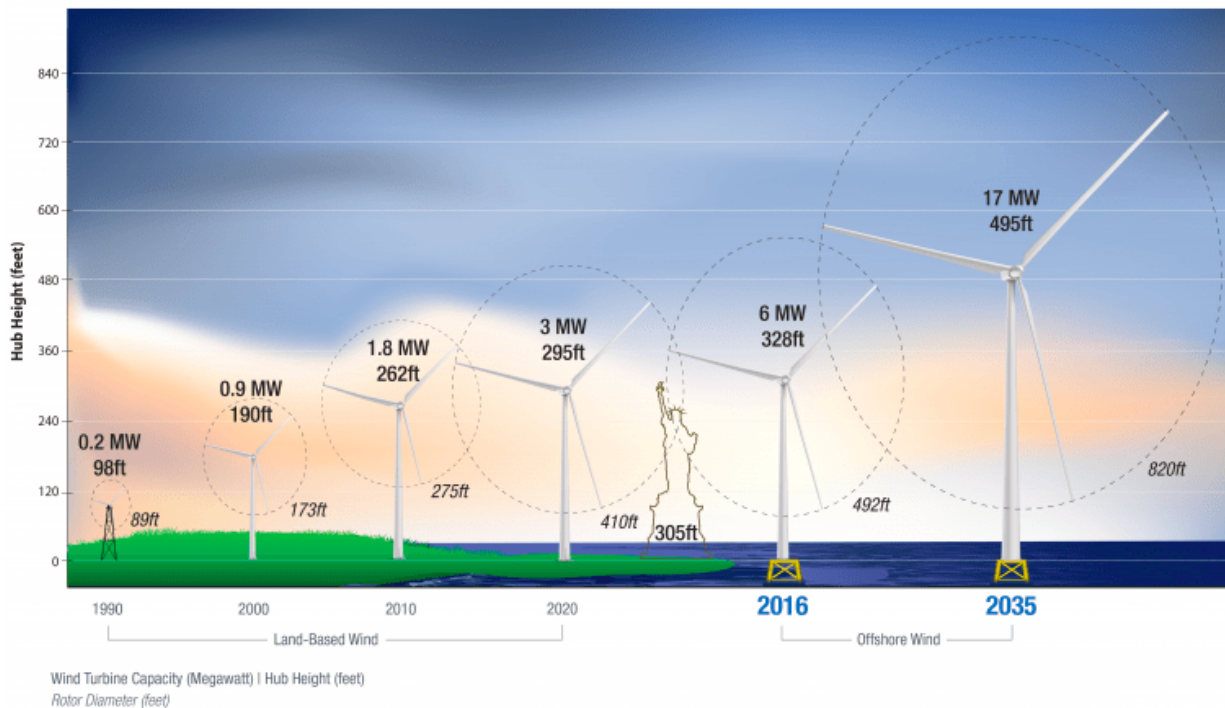


**Figure 2:** Evolution of wind turbines [10]

The evolution of wind turbines encompasses more than just their size and power generation capabilities; it also involves their geographical placement. The first operating wind farm can be tracked back to Vineby in Denmark in 1991 [11]. Since then, a significant number of offshore wind turbines have been assembled, with numerous future installations anticipated in the years ahead. The offshore environment holds tremendous potential for wind energy development due to several compelling factors. As per August 2022, Hornsea 2 is the largest offshore wind turbine farm, 89 km off the Yorkshire Coast in England. Figure 3 shows the farm that consists of a total of 165 turbines, and generating 1,3 GW [12].

Offshore environments experience stronger wind conditions compared to land areas. Faster wind speeds allow for substantially greater energy production. Wind speeds off the coast are typically more consistent than on land. A more consistent wind supply translates into a more stable source of energy. Offshore wind farms share many of the same benefits as land-based wind farms, including the ability to produce renewable energy, the lack of water usage, the provision of a domestic energy supply, the creation of jobs, and the absence of greenhouse gas emissions [13].

**Figure 3:** Hornsea 2 offshore wind farm [12]

However, offshore wind turbines have some downsides. It can be expensive and challenging to construct and manage offshore wind farms. Particularly in deeper waters, with the difficulty of constructing strong and stable wind farms. These difficulties can be overcomed by floating wind turbines. Wind turbines can sustain damage from rain, wave action and even very high winds, especially during severe storms or hurricanes. This will accelerate the wear which may result in more frequent maintenance being required. Manufacturing and installing power cables beneath the seabed to transport electricity back to land can also be quite expensive. It has not been fully understood how offshore wind farms affect birds and marine life. This is something that will require more research. Offshore wind farms constructed within sight of the coastline would not be well-liked by the locals, which could harm tourism and property prices as well [13].

## 2.2. Components

The 3-blade horizontal wind turbine is as mentioned earlier the most commonly used wind turbine. It usually consists of a tower, housing the power cable, a nacelle containing among other things the generator and yaw system, rotor and blade as shown in Figure 4. Since a wind turbine can be exposed to high wind speeds, safety and efficiency are essential. The wind turbine should be positioned with regard to the wind to generate as much power as possible, and avoid any damage the equipment. This could happen if the wind is too strong, too little oil or the temperature is too high on the bearings. Therefore, a wind turbine consist of many sensors to monitor the conditions [14].

The anemometer is one of these sensors, measuring the wind speed. Wind speed is often averaged over a brief period of time since wind speeds are not constant; there are gusts and long pauses. The anemometer measures the changes, from which wind speed is determined and sent to the controller [16]. The controller allows the wind turbine to start at wind speeds of approximately 3-5 meters per second. When wind speeds exceed 24-29 meters per second, the controller shuts the turbine off in order to protect various turbine components from harm [17]. Another important component for safety and efficiency is the nacelle. The nacelle is a section that houses section the gearbox, brake, low- and high-speed shafts, generator, and control electronics. The nacelle's controlling mechanism includes information on wind speed and direction, rotor speed, and generator capacity. As a result, the controller allows the turbine to move in the direction of the wind with the aid of the yaw mechanism [18]. Over the rated wind speeds, the yaw system can be employed for power regulation. This can be accomplished by reducing the area of the rotor that is swept into the incoming wind. By minimizing fatigue loads or shielding the wind turbine from high stresses in extreme wind conditions, the yaw system help reduce overall load [19].
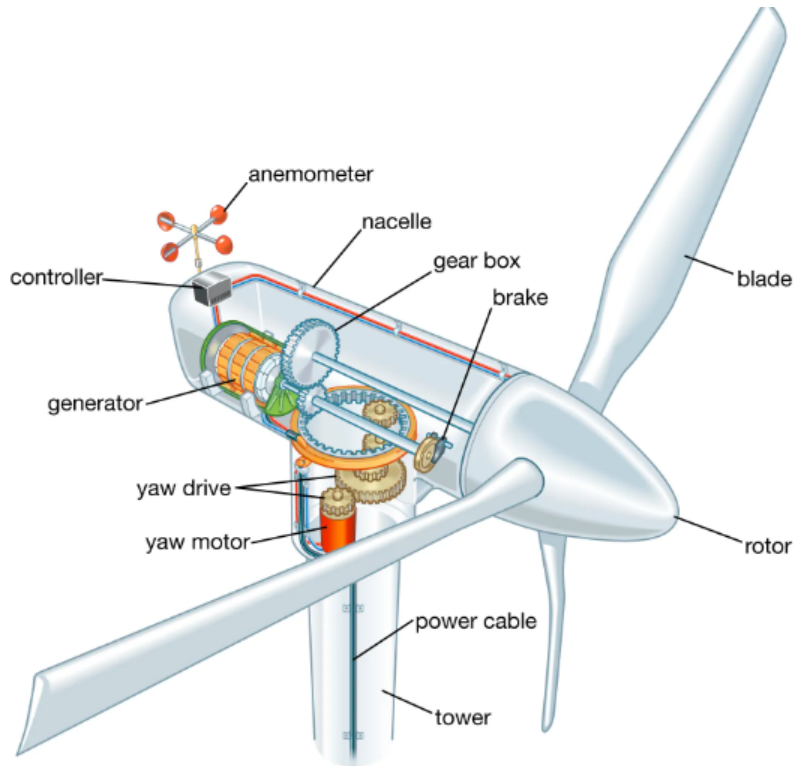
**Figure 4:** Components of a wind turbine [15]

In terms of performance and cost of the wind power system, rotor blades are the most crucial components of a wind turbine. Performance is directly impacted by the rotor blade's shape since it determines how wind kinetic energy is converted to mechanical energy. Based on aerodynamic principles, these kinds of wind turbines are built with blades that have a high lift to drag ratio. Wind turbine blades encounter various forces while in operation, as gravitational, aerodynamic, and centrifugal forces. The selection of the number of blades for a wind turbine is based on several key considerations rooted in aerodynamic effectiveness, component prices, and system reliability [20]. The rotor is connected to the gearbox that is frequently used to raise the rotating speed from the main shaft's low speed to the high-speed shaft. The high speed shaft propels the electrical generator. In the generator, copper windings rotate through a magnetic field to generate electrical energy [17].

The tower, which can be made of tubular steel, supports the turbine's frame and house the power cable. Towers are typically delivered in three sections and put together on-site. Taller towers allow turbines to catch more energy and produce more electricity since wind speed rises with height. At 30 meters or higher, winds are also less turbulent [17]. Wind turbine towers are cylindrical because they are designed to resist the loads from the wind and the weight of the turbine blades and nacelle. A cylindrical shape provides the most efficient use of materials, making it the most cost-effective and structurally sound option for towers. Additionally, cylindrical shapes are better at withstanding wind loads than other shapes like square or rectangular. The circular shape allows the tower to deflect slightly when subjected to wind loads, which helps to distribute the load evenly across the tower and reduces the risk of damage or failure. Moreover, the circular shape of the tower is aerodynamically efficient, meaning it has minimal wind resistance or drag, and can provide better stability for the wind turbine overall. This is important as it helps to minimize the forces on the tower and prevent fatigue or damage over time [21].

## 2.3. Function

A wind turbine uses the aerodynamic force of the rotor blades to convert wind energy into electricity. The air pressure on one side of the blade falls as wind passes across it. Both lift and drag are produced by the different air pressure on the blade's two sides as shown in Figure 5. The rotor spins because the force of the

lift is greater than the force of the drag. A shaft and a set of gears that speed up the rotation and enable a physically smaller generator, are used to link the rotor to the generator. Electricity is produced as a result of the conversion of aerodynamic force into generator rotation [22].
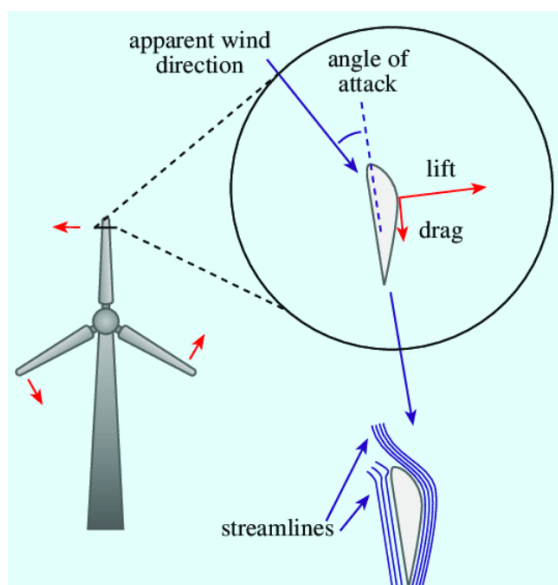


**Figure 5:** Functionality of a wind turbine: wind flow and aerodynamic forces [23]

The advancement of wind turbine technology has facilitated the construction of larger turbines with increased energy generation capabilities. Consequently, the generators have also grown in size, leading to assumptions of improved efficiency. Nevertheless, every wind turbine generator encounters an upper limit in its capacity to convert wind energy into usable power, known as the Betz Limit. The Betz limit, proposed by German physicist Albert Betz in 1919, represents the theoretical maximum efficiency achievable by a wind turbine and is calculated to be 59,3%. This signifies that the turbine can harness a maximum of 59,3% of the kinetic energy present in the wind to drive its rotation and generate electricity. In practical applications, turbine efficiencies typically range between 35% and 45%, falling short of the Betz limit [24].

## 2.4. Material

According to a report from the National Renewable Energy Laboratory, the composition of wind turbines varies depending on the make and model. The predominant materials used in wind turbines are as follows: steel comprises 66-79% of the total turbine mass, fiberglass, resin, or plastic accounts for 11-16%, iron or cast iron ranges from 5-17%, copper constitutes approximately 1%, and aluminium makes up 0-2% of the total mass [25]. The turbine blade is made from a composite material comprised of glass fabric and carbon fiber and impregnated with liquid plastic resin. Earlier, aluminium was used in the blades of smaller vertical, rotors. However, engineers came to the conclusion that using aluminium resulted in the blades being too heavy [26].

A staggering 85% of turbine parts, including steel, copper wire, electronics, and gears, may be recycled or used again. The fiberglass and carbon fiber blades, however, are still challenging to get rid of. The hurricane-resistant blades are difficult to crush, recycle, or use for another purpose. Consequently, the demand for alternative materials, particularly bio-based fibers, is crucial in regions where expansive grasslands are not easily available. Some blades are burned in power plants or cement-making kilns in the European Union, where there are tight restrictions on what can be disposed of in landfills. However, the blades have a poor and inconsistent energy content, and burning fiberglass releases pollutants. Most of the tens of thousands of outdated blades from steel towers all around the world, will end up in landfills as shown in Figure 6 [27].

**Figure 6:** Landfill disposal of wind turbine blades [27]

## 2.5. New design

World Wide Wind is actively engaged in the development of the next generation of floating offshore wind technologies. This Norwegian-based company is dedicated to introduce innovative solutions and cutting-edge technology, particularly in the form of counter-rotating VAWT as shown in Figure 7. These turbines offer substantial advancements over existing VAWT technology, demonstrating World Wide Wind's commitment to be one of the innovation leaders in the field of offshore wind energy [28].



**Figure 7:** World Wide Wind's innovative offshore wind turbine design [28]

The conceptual sketch shown in Figure 8 represents World Wide Wind's offshore wind turbine design, with a specific focus on the joint between the mast and the turbine blade. This area is highlighted within the sketch to indicate its significance as the main focus of the master thesis. By narrowing the scope to this specific joint, the thesis aims to delve deeper into the analysis, design, and optimization of this crucial connection. The selected focus area allows for a more detailed examination of the structural integrity, load distribution, and performance characteristics at this critical interface.
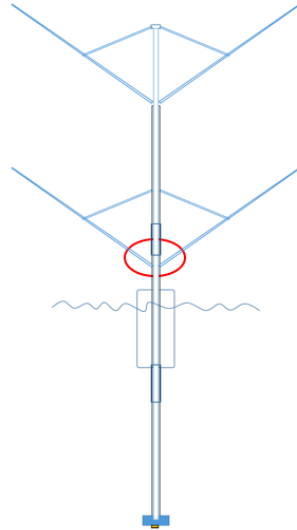
**Figure 8:** Conceptual sketch of World Wide Wind's offshore wind turbine design with emphasis on focus area [29]

The turbine floats due to a floater, with the generator being below sea-level. There are a total of 6 turbine blades, 3 are attached to both the outer and inner masts [29]. On the inside, between the inner and outer mast, rotary bearings are found. In motion systems, rotary bearings are a common component. They are utilized in pumps, fans, pulleys, fans, and motors. Rotary bearings are essentially always present whenever a shaft is spinning in order to reduce friction and support radial or axial loads. Many rotary bearing varieties exist, including models created for particular environments, mounting arrangements, and uses [30].

Currently, World Wide Wind are in a product development period where prototypes are being made in 6082-T6 aluminium. The turbine blades are attached with bolts to the mast as well as a bracket to the bracing on top to distribute the load. World Wide Wind's current design has a 55° angle between the mast and blade. This is a design choice. A larger angle would result in a greater swept area, which could make the turbine heavier and more expensive. A smaller angle could result in a smaller swept area and therefore less energy [29].

# 3. Joining methods

Joining aluminium components can be done through a variety of methods. The specific method used depends on factors such as the application, the thickness of the aluminium, and the desired properties of the joint. It is assumed that a bracket will be used to join the mast and the turbine blade together, as shown in Figure 9. Two major joining techniques will be compared; standard component that is welded or bolted and special purpose extrusion design. These are some of the applicable joining methods to join the bracket to the mast that will be presented in this chapter. In addition, calculations and simulations will be carried out.
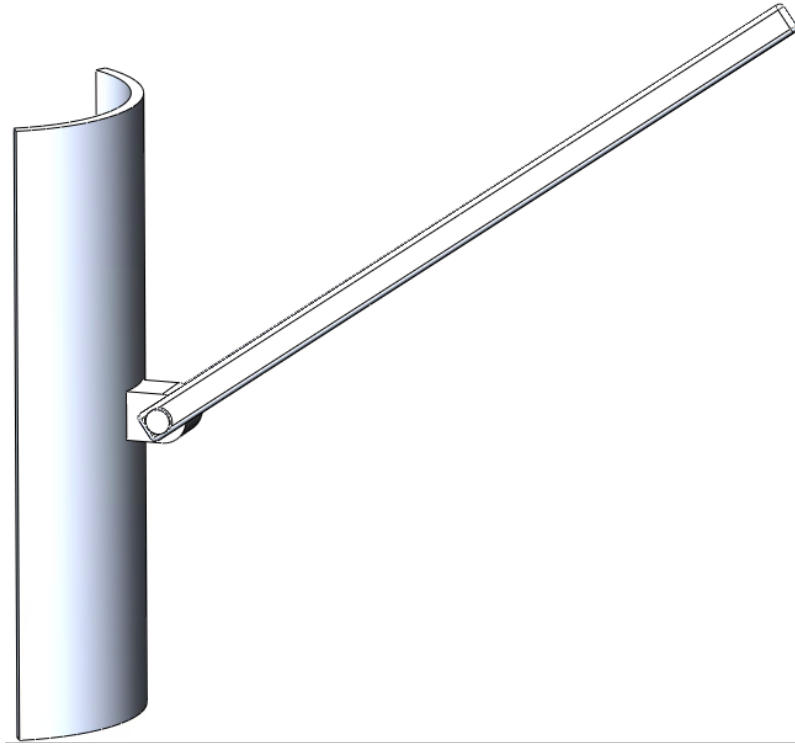


**Figure 9:** 3D model of mast and turbine blade connection

Figure 10 shows a close-up image of the parts that will be used to create the joint. The turbine blade is attached to the bracket and fixed by a bolt. It is how the bracket is joined to the mast that will be looked into.
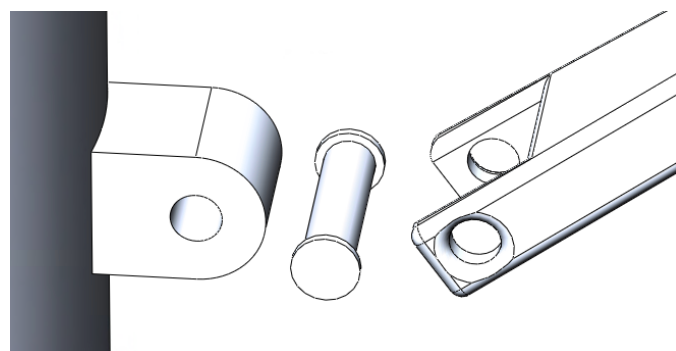


**Figure 10:** Close up view of the 3D modeled components joining the mast and turbine blade

## 3.1. Relevant forces and load

There are some differences in experienced forces for an offshore wind turbine compared to a wind turbine on land. A fixed wind turbine on land is constrained by its foundation, which restricts its movement to only rotation around a single axis. In contrast, a floating wind turbine has additional degrees of freedom due to its movement in the water. This property allows for movement not only in terms of rotation but also in translation and various other directions, thereby influencing the forces exerted on the object by the wind. Considering the unfixed nature of the wind turbine, allowing it to rotate freely in the water, it is assumed that the influence of wind-induced loads can be considered negligible. This results the joint experiencing two forces; centrifugal (Fx) and gravitational (Fy).

In the field of materials science and engineering, the fatigue life of a specimen is described as the number of loading cycles it can withstand before experiencing failure. Cycled stresses, residual stresses, material characteristics, internal flaws, grain size, temperature, design geometry, surface quality, oxidation, corrosion, etc. all have an impact on fatigue life [31]. Figure 11 shows an estimated SN curve for 6082-T6 aluminium. An SN curve, is a graphical representation that explains the relationship between the applied cyclic stress (S) and the number of cycles to failure (N) for a material.
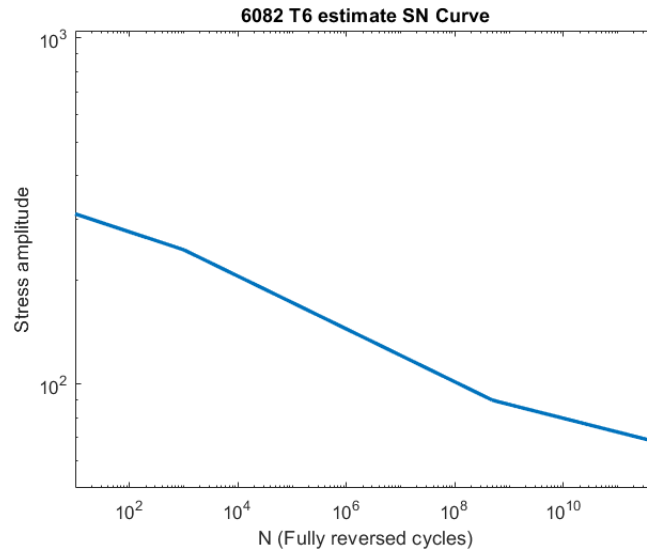


**Figure 11:** Estimated SN curve for 6082-T6 aluminium [32]

While the consideration of fatigue life is crucial for real-life applications where components and structures experience cyclic loading, the thesis will focus on static loads. By assuming static loads, the focus will be towards analysing the structural integrity, load-carrying capacity, and factors like safety margins. Although fatigue life may not be taken into account for the calculations and simulations, it remains an important aspect to be mindful of in practical applications where cyclic loading is common.

Documentation from World Wide Wind states that the bracing is required to handle 40 kN. Through the utilization of this resultant force, it becomes possible to decompose and determine the horizontal and vertical forces applied on the bracket. The angle between mast and turbine blade is 55 degrees as stated earlier. The decomposing of the of the resultant force is showed in Figure 12 with the calculations showed in equation 1 and 2.

**Figure 12:** Load distribution and decomposition at 55 degree

$$cos\alpha = \frac{Fx}{F} \implies Fx = 40kN \cdot cos22° = 37,1kN \tag{1}$$

$$sin\alpha = \frac{Fy}{F} \implies Fy = 40kN \cdot sin22° = 15,0kN \tag{2}$$

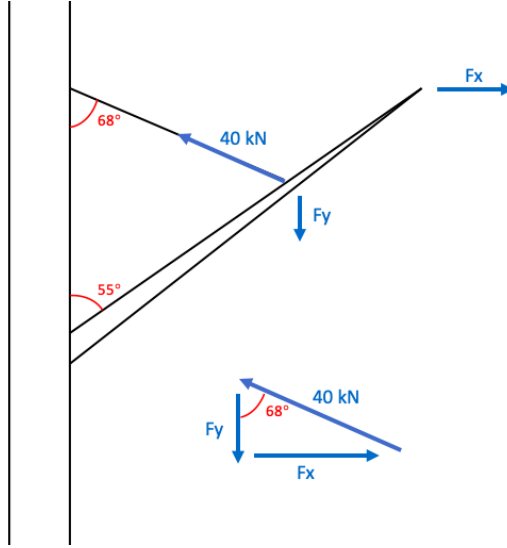These forces will be used in the calculations and simulations for the different joining methods.

## 3.2. Welding

Welding is a very common joining method. There are many different welding techniques, two of them are called TIG and MIG. Tungsten Inert Gas (TIG) welding, also known as Gas Tungsten Arc Welding (GTAW), involves the use of a pointed tungsten electrode to create an arc. A shielding gas, typically pure argon, is introduced through a gas nozzle surrounding the electrode. In some cases, additional material can be fed as a wire in front of the arc and molten pool, known as cold wire addition. One notable advantage of this method is that the amount of additive remains independent of the welding current, including the melting of the base material, making it valuable in certain applications [33].

When it comes to welding aluminium, TIG welding poses a specific challenge. With the positive pole connected to the workpiece, the oxide layer is not effectively removed. As a result, Metal Insert Gas (MIG) welding, also referred to as Gas Metal Arc Welding (GMAW), has gained prominence as the most economically significant welding technique. In MIG welding, an arc is created by continuously feeding a solid wire through a shielding gas, predominantly argon, from a gas nozzle. The gas, electrode wire, and power cable are typically integrated into a single cable and fed to the welding gun. The wire feeder regulation is often located within the current source, resulting in the regulation of the current itself [33].

Welding results in in a Heat-Affected Zone (HAZ) which is noticeably affected by the heat input from the welding process [33]. The material characteristics for aluminium near to the weld will significantly change. The HAZ is for example typically 30 to 50% weaker than the base material when fusion-welding high-strength 6xxx series alloy [34]. Figure 13 shows a comparison between a stress-strain curve for two aluminium alloys and their HAZ. The graph shows that all four cases have a similar elastic behaviour to a strain-value of about 0,002. There the two HAZ-graphs reaches the yield point and the material has entered its plastic deformation. This happens a bit later for 5083 without HAZ, and even later for the 6082 without HAZ. For the two alloys, the biggest difference for the parent material compared to the HAZ is for 6082.
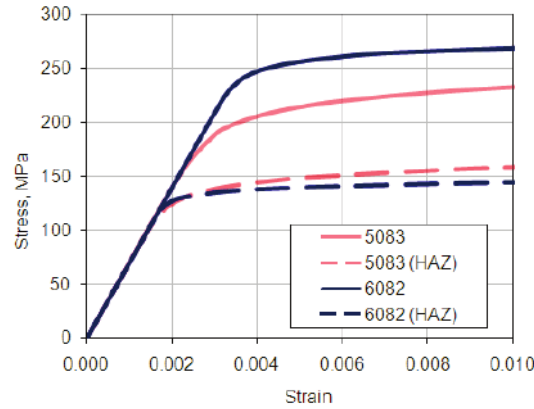
**Figure 13:** Stress-strain curves illustrating the material behavior of aluminium alloys 5083-H116 and 6082-T6 in both the parent metal and the HAZ [35]

The HAZ cause a decrease in hardness relative to the surrounding material. This phenomenon is visible in Figure 14, as illustrated in the hardness profile across the distance from the weld centerline for 6061-T651 aluminium, applying an ER4042 filler wire. These changes in properties in the HAZ, shows the importance of considering the HAZ characteristics when assessing the weld's mechanical performance.



**Figure 14:** The variation in hardness across a weld in 6061-T651 aluminium, with ER4043 filler wire [36]

### 3.2.1. Weld calculation

Figure 15 is a 3D-model that visualizes how the bracket joined to the mast through welding could look like.



**Figure 15:** 3D model of a welded bracket joining the mast

13

It would be natural to assume that a fillet weld would be the best for this case. However, according to Eurocode 9, Section 8.6.3.2.1, "Full penetration butt welds should be applied for primary load-bearing members". And since this joint can be considered primary load-bearing, full pen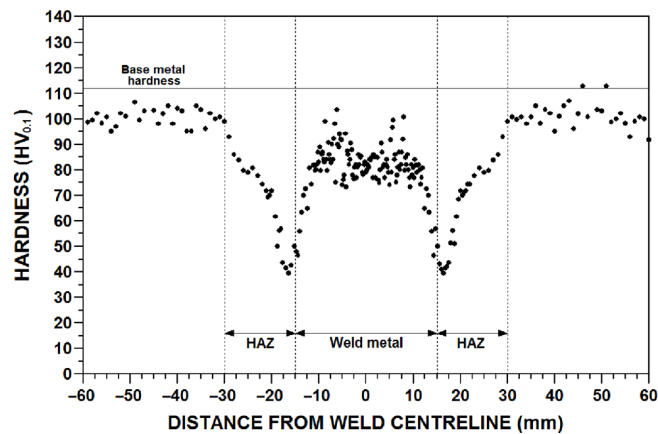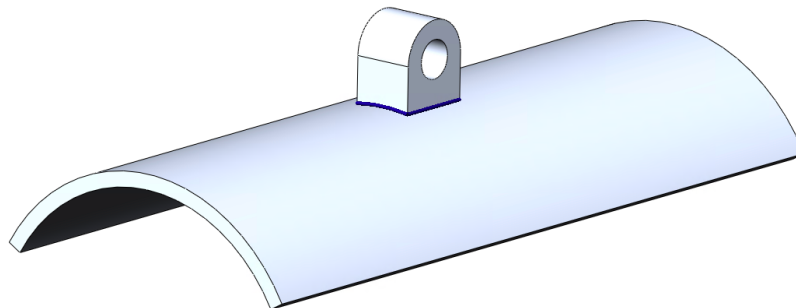etration weld will be considered further. Information, formulas and values used in this subsection are found in NS-EN 1999-1-1:2007 [37].

It is important to mention that the design guidance is for structures loaded with mainly static loads. This would not necessary be the case for a joint on a wind turbine. Dynamic loads and fatigue life needs to be taken into consideration for this kind of application. To simplify the calculation, the mast and bracket are assumed flat with the load being static.

The HAZ should be considered for heat-treatable alloys in temper T4 and above (6xxx and 7xxx series) and non-heat-treatable alloys in any work-hardened condition (3xxx, 5xxx, and 8xxx series). It is important to consider the degree and dimensions as a result of HAZ softening. If the welds have a higher design strength than the material in the HAZ, the deformation capacity of a welded junction can be increased. With the exception of the strength in the HAZ, the strength in the weld metal is typically lower than the parent metal in welded connections. The strength of the weld metal will be substantially affected by the filler metal. Characteristic strength for 6082 aluminium allow with two different filler metals are presented; 5356 and 4043A. It is chosen to use the 4043A in the calculations.

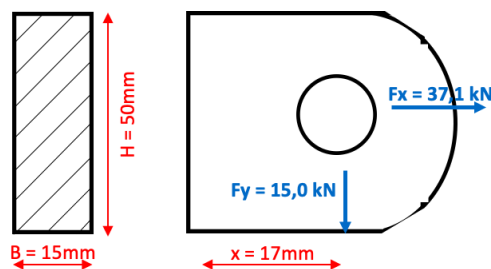Figure 16 shows the cross section of the bracket with dimensions that will be used in the calculation.



**Figure 16:** Cross section of welded aluminium bracket

NS-EN 1999-1-1:2007 is based on dimensioning with partial factors, at the limit state design. The capacity on the material side is reduced by $\gamma_{Mw}$, which is a partial safety factor for welded joints. This is set to 1,25 for the dimensioning of welds according to this standard. Partial safety factors are applied to the material properties and resistance of the weld. These factors account for uncertainties in material properties, manufacturing processes, and other factors that can affect the strength and performance of the weld. In addition, the load is increased by using a load factor, $\gamma_L$. Load factors are applied to the loads or actions acting on the structure to account for uncertainties in their magnitude or occurrence. These load factors represent a safety margin by increasing the design loads to ensure that the structure can withstand them without reaching critical conditions. The specific load factors to be used depend on the type of load and the design situation. This is typically in the order of 1,3 – 1,5. The load factor will be set at 1,5 [38].

**Check of weld**

In addition to the horizontal force, will the bending moment caused by the vertical force also contribute to tensile stress in the weld. The bending moment will result in tensile stresses in the upper part and compressive stresses in the lower part of the weld. Formula 3 shows how to check the tensile stress in the weld. The characteristic strength values of weld metal, $f_w$, for 6082 with filler metal 4043A is 190 N/$mm^2$.

$$\sigma_{\perp Ed} \leq \frac{f_w}{\gamma_{Mw}} \tag{3}$$

To calculate the total tensile stress in the weld, formula 4 is used.

$$\sigma_{\perp Ed} = \frac{F_x \cdot \gamma_L}{A} + \frac{M \cdot c \cdot \gamma_L}{I} = \frac{F_x \cdot \gamma_L}{A} + \frac{F_y \cdot x \cdot c \cdot \gamma_L}{b \cdot h^3} \tag{4}$$

$$\sigma_{\perp Ed} = \frac{37087,35N \cdot 1,5}{15mm \cdot 50mm} + \frac{14984,26N \cdot 17mm \cdot 25mm \cdot 1,5}{\frac{15mm \cdot (50mm)^3}{12}} = 74,17\frac{N}{mm^2} + 61,14\frac{N}{mm^2} = 135,31\frac{N}{mm^2}$$

$$135,31\frac{N}{mm^2} \leq \frac{190\frac{N}{mm^2}}{1,25} = 152\frac{N}{mm^2} \rightarrow OK$$

To check the shear stress in the weld, formula 5 will be used.

$$\tau_{Ed} \leq 0,6 \cdot \frac{f_w}{\gamma_{Mw}} \tag{5}$$

To calculate the shear stress in the weld, formula 6 is used.

$$\tau_{Ed} = \frac{F_y \cdot \gamma_L}{A} \tag{6}$$

$$\tau_{Ed} = \frac{14984,26N \cdot 1,5}{15mm \cdot 50mm} = 29,97\frac{N}{mm^2}$$

$$29,97\frac{N}{mm^2} \leq 0,6 \cdot \frac{190\frac{N}{mm^2}}{1,25} = 91,2\frac{N}{mm^2} \rightarrow OK$$

To check the combined stress for shear and tensile stress in the weld, formula 7 is used.

$$\sqrt{\sigma^2_{\perp Ed} + 3 \cdot \tau^2_{Ed}} \leq \frac{f_w}{\gamma_{Mw}} \tag{7}$$

$$\sqrt{(135,31\frac{N}{mm^2})^2 + 3 \cdot (29,97\frac{N}{mm^2})^2} = 144,93\frac{N}{mm^2} \leq \frac{190MPa}{1,25} = 152\frac{N}{mm^2} \rightarrow OK$$

**Check of HAZ**

For the HAZ, it is assumed that the both shear and tensile stresses are calculated exactly the same as for the weld. It is however checked against a lower characteristic strength, $f_{u,haz}$, at 185 N/$mm^2$. To check the tensile stress in the HAZ, formula 8 will be used.

$$\sigma_{haz,Ed} \leq \frac{f_{u,haz}}{\gamma_{Mw}} \tag{8}$$

$$\sigma_{haz,Ed} = \frac{37087,35N \cdot 1,5}{15mm \cdot 50mm} + \frac{14984,26N \cdot 17mm \cdot 25mm \cdot 1,5}{\frac{15mm \cdot (50mm)^3}{12}} = 74,17\frac{N}{mm^2} + 61,14\frac{N}{mm^2} = 135,31\frac{N}{mm^2}$$

$$135,31 \leq \frac{185\frac{N}{mm^2}}{1,25} = 148\frac{N}{mm^2} \rightarrow OK$$

To check the shear stress in the HAZ, formula 9 is used.

$$\tau_{haz,Ed} \leq \frac{f_{v,haz}}{\gamma_{Mw}} = \frac{\frac{f_{u,haz}}{\sqrt{3}}}{\gamma_{Mw}} \tag{9}$$

$$\tau_{haz,Ed} = \frac{14984,26N \cdot 1,5}{15mm \cdot 50mm} = 29,97\frac{N}{mm^2}$$

$$29,97\frac{N}{mm^2} \leq \frac{\frac{185\frac{N}{mm^2}}{\sqrt{3}}}{1,25} = 85,45\frac{N}{mm^2} \rightarrow OK$$

To check the combined shear and tensile stress in the HAZ, formula 10 is used.

$$\sqrt{\sigma^2_{haz,Ed} + 3 \cdot \tau^2_{haz,Ed}} \leq \frac{f_{u,haz}}{\gamma_{Mw}} \tag{10}$$

$$\sqrt{135,31\frac{N}{mm^2}^2 + 3 \cdot 29,97\frac{N}{mm^2}^2} = 144,93\frac{N}{mm^2} \leq \frac{185MPa}{1,25} = 148\frac{N}{mm^2} \rightarrow OK$$

Considering the tensile and shear stresses resulting from the applied loads, the weld joint, as well as the HAZ, will remain intact and capable of withstanding the forces. By having profile design in mind, the welding can be simplified which could result in a higher strength. This could be consideration of root support, material compensation, joint processing as well as reduced number of welds [39]. If the weld however had failed, in theory, it could be possible to increase the capacity of the weld by adding external fillet welds. This is a combination weld, called full penetration T-weld with superimposed fillet welds. Such a solution will increase the capacity in the weld and in the HAZ towards the mast, but will not increase the capacity of the HAZ in the bracket itself. For a real construction, it could be beneficial to consider adding stiffeners or smoothing the transition from bracket to mast. This is typically areas where local stress can appear, regardless of whether the weld is correctly dimensioned. This will also have a major impact on fatigue life [38].

### 3.3. Bolt connection

Bolted connections are utilized more often than other types of connections. The method requires no specialized equipment, and bolts are incredibly simple to use. This is especially true because stronger bolts have been developed, making it possible to join structural steel in an easier and more reliable way. However, bolt connections needs drilling and hole-adjustment during installation which reduces the manufacturability. Cutting of the holes may weaken the steel members and increase the consumption of steel materials, as a result of member overlap. Additionally, this will increase the workload during construction. The failure of the bolted connections may be caused by a variety of factors, including overloading, excessive torque, and corrosion damage [40].

The possibility of changes in tightness as a result of thermal expansion is a problem for steel bolts. This factor is however eliminated using aluminium bolts. The material of the aluminium bolt is selected to complement the material forming the components to be joined. When using bolts, there are several guidelines that should considered. By placing hard aluminium washers under the bolt and nut heads, will it be possible to prevent too high pressure on the surface of the aluminium when the fastener is tightened. Bolts that are regularly undone and tightened again can cause the component to wear out the thread on the bolt. The aluminium bolts used in joints exposed to moisture should be sealed to prevent corrosion [41].

Overall, bolt connections can be an effective method for joining, but careful design and consideration of potential issues is necessary to ensure the long-term integrity and reliability of the joint. Figure 17 is a 3D model that visualizes how the bracket joined to the mast through bolt connection could look.
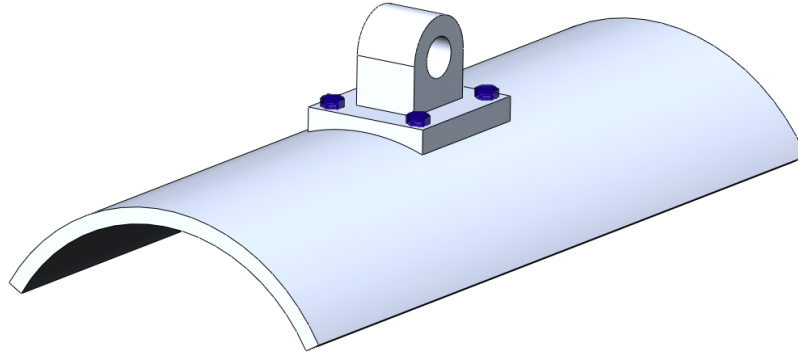
**Figure 17:** 3D model of a bolted bracket joining the mast

### 3.3.1. Bolt calculation

Once again, a static load is assumed and will therefore calculate linear elastic. For more detailed calculations, dynamic load and fatigue life should be considered. Just as in the welding calculations, it is assumed that all surfaces are flat, and not curved as it would be for this application. Information, formulas and values in this subsection are based on Eurocode 9 in NS-EN 1999-1-1:2007 [37].

Three different loads will be checked for the bolts; shear, tension and combined shear and tension. For shear connections, category A (bearing type) will be used. This category requires no preloading and all bolt grades from 4.6. to 10.9 are allowed. For tension connections, category D (non-preloaded) will be used. This category states that all bolt classes from 4.6. to 10.9 are allowed.

A total of four M16 8.8. bolts will be used, with the assumption that the load is evenly distributed over the four bolts. For the edge distance to bolt, both minimum, regular and maximum distance are provided in the standard. The minimum distance is based on strength, while the maximum is based on corrosion. Regular distance is chosen to use with $e_1$ equal to $2,0d_0$, $e_2$ equal to $1,5d_0$ and $p_1$ equal to $2,5d_0$. These represents the distance from center of the hole to the edge both horizontally and vertically, as well as the distance between the holes. A load factor of 1,5 will be used for safety reasons. And for uncertainties in the material, a material factor for bolt connections, $\gamma_{M2}$, at 1,25 is added. It is assumed that block tearing will not be a problem.

Figure 18 shows the cross section of the bolted aluminium bracket with dimensions that are used in the calculations.
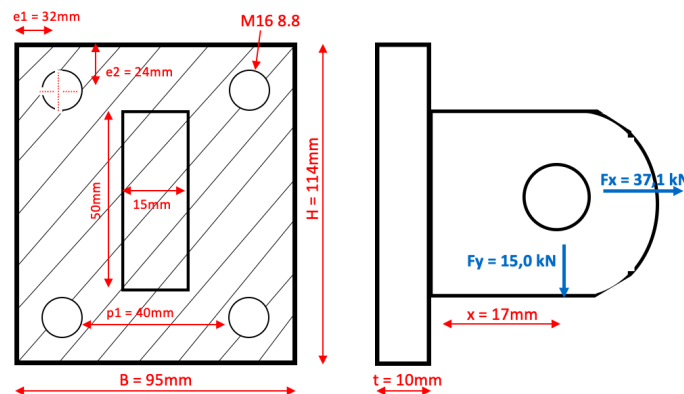


**Figure 18:** Cross section of bolted aluminium bracket

**Category A: Shear connections**

The design shear force per bolt for the ultimate limit state should be less than the design shear resistance per bolt and the design bearing resistance per bolt as shown in formula 11 and 12.

$$F_{v,Ed} \leq F_{v,Rd} \tag{11}$$

$$F_{v,Ed} \leq F_{b,Rd} \tag{12}$$

To calculate the shear force per bolt, formula 13 is used.

$$F_{v,Ed} = \frac{F_y \cdot \gamma_L}{4} \tag{13}$$

$$F_{v,Ed} = \frac{14984,26 \cdot 1,5}{4} = 5619,1N$$

To calculate the design shear resistance per bolt, formula 14 is used.

$$F_{v,Rd} = \frac{\alpha_v \cdot f_{ub} \cdot A}{\gamma_{M2}} \tag{14}$$

For aluminium bolts $\alpha_v$ is 0,5. The characteristic ultimate strengths of the bolt material, $f_ub$, only has two different thicknesses for 6082-T6 for this standard. These are not necessary accurate, so an average value will be used at 315 MPa. A is the tensile stress area of the bolt which is $157mm^2$ for M16 bolts [42]. It is assumed that the shear plane of the bolt is through the threaded area and that A and $A_s$ are equal.

$$F_{v,Rd} = \frac{0,5 \cdot 315MPa \cdot 157mm^2}{1,25} = 19782N$$

To calculate the design bearing resistance per bolt, formula 15 is used.

$$F_{b,Rd} = \frac{k_1 \cdot \alpha_b \cdot f_u \cdot d \cdot t}{\gamma_{M2}} \tag{15}$$

Perpendicular to the direction of the load transfer, $k_1$ is the smallest value of $2,8e_2/d_0 - 1,7$ and 2,5. This results in $k_1$ being 2,5. $\alpha_b$ is the smallest value of $\alpha_d$, $f_{ub}/f_u$ or 1,0, where $\alpha_d$ is equal to $e_1/3d_0$ for end bolts. This results in $\alpha_b$ being 0,67. The characteristic ultimate strength of the member material, $f_u$, is 310 MPa for extruded 6082-T6 alloy. The nominal diameter, d, for M16 bolts are 16mm. For the thickness, t, the smallest value of the flange plate and mast is used. Both of these are 10mm, thus this is also the value used.

$$F_{b,Rd} = \frac{2,5 \cdot 0,67 \cdot 310MPa \cdot 16mm \cdot 10mm}{1,25} = 66464N$$

$$5619,1N \leq 19782N \rightarrow OK$$

$$5619,1N \leq 66464N \rightarrow OK$$

**Category D: Tension connections**

The design tensile force per bolt for the ultimate limit state should be less than the design tension resistance per bolt and the design resistance for punching resistance as shown in formula 16 and 17.

$$F_{t,Ed} \leq F_{t,Rd} \tag{16}$$

$$F_{t,Ed} \leq B_{p,Rd} \tag{17}$$

To calculate the design tensile force per bolt for the ultimate limit state, formula 18 is used.

$$F_{t,Ed} = \frac{F_x \cdot \gamma_L}{4} + \frac{M \cdot \gamma_L}{c \cdot 2} \tag{18}$$

$$F_{t,Ed} = \frac{37087,35N \cdot 1,5}{4} + \frac{14984,26N \cdot (17+10)mm \cdot 1,5}{56mm \cdot 2} = 19326,17N$$

To calculate the design tension resistance per bolt, formula 19 is used.

$$F_{t,Rd} = \frac{k_2 \cdot f_{ub} \cdot As}{\gamma_{M2}} \tag{19}$$

For aluminium bolts, $k_2$ is 0,5.

$$F_{t,Rd} = \frac{0,5 \cdot 315MPa \cdot 157mm^2}{1,25} = 19782N$$

To calculate the design resistance for punching resistance, formula 20.

$$B_{p,Rd} = \frac{0,6 \cdot \pi \cdot d_m \cdot t_p \cdot f_u}{\gamma_{M2}} \tag{20}$$

The mean of across points and across flats dimensions of the bolt head or nut, $d_m$, is found in [43]. The thickness of the flange plate will be regarded as $t_p$.

$$B_{p,Rd} = \frac{0,6 \cdot \pi \cdot 25,375mm \cdot 10mm \cdot 310MPa}{1,25} = 118620,3N$$

$$19326,17N \leq 19782N \rightarrow OK$$

$$19326,17N \leq 118620,3N \rightarrow OK$$

**Combined shear and tension**

To check the combined shear and tension, formula 21 is used with the values calculated above.

$$\frac{F_{v,Ed}}{F_{v,Rd}} + \frac{F_{t,Ed}}{1,4F_{t,Rd}} \leq 1,0 \tag{21}$$

$$\frac{5619,1N}{19782N} + \frac{19326,17N}{1,4 \cdot 19782} = 0,98 \leq 1,0 \rightarrow OK$$

With these calculations, the values are acceptable and the model will withstand the load applied. It is more common to use steel bolts, these also have a much higher ultimate strength. Steel bolts in 8.8 have an ultimate strength of 800 MPa. Where fasteners are required to carry an applied tensile force, they should be proportioned to also resist the additional force due to prying action [37]. This is not taken to consideration here, but should be taken into account for implementation of bolt connections.

## 3.4. T-track

T-track can be directly extruded with the right shape, and therefore do not loose any strength like welding. Extruded aluminium profiles are made from extruded billets, which are made from either primary aluminium, recycled aluminium, or a combination of the two. The extruded billets are available in a variety of different alloys and specifications that are adjusted to demands and requirements. It is cast in lengths up to 7 meters. Extruded billets typically range in size from 400 to 1000 mm in length and 150 to 300 mm in diameter, depending on the extrusion press and length of the profile. The aluminium bolt is heated up to between 450 and 500°C and forced through a profile tool under a pressure of 1 200–7 000 tonnes. The cross-section of the profile is represented by the opening in the tool. The extrusion speed varies depending on the alloy, size, extrusion press and complexity of the profile, but the typical range is 5 to 50 m/min. Figure 19 illustrates the extrusion principle. Depending on the size, shape, alloy, and desired qualities of the profile, it is either cooled using air or water when it is fed onto an output and cooling table after being extruded. The profiles are stretched to relieve any material stress and achieve straight profiles. After, the profiles are trimmed to the proper lengths and shipped for heat curing. Curing takes place for 4 to 8 hours at a temperature of roughly 190°C in a curing oven. The profiles are then ready for further processing or to be sent to the customer after one last check [39].
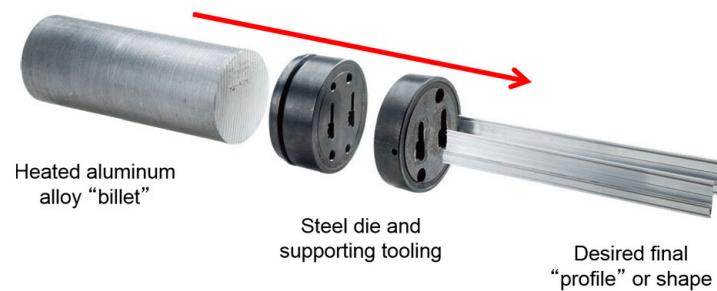


**Figure 19:** Extrusion process for manufacturing aluminium profiles [44]

The 6xxx series of aluminium alloys are generally considered the best class of alloys for extrusion due to their favorable combination of extrudability, mechanical properties, and corrosion resistance. This series includes alloys such as 6063, 6061, and 6082, which are widely used for extrusion applications. The 6xxx series alloys are aluminium-magnesium-silicon alloys. They offer excellent formability, allowing for the production of complex shapes and profiles with good surface finish. These alloys also exhibit good strength, corrosion resistance, and weldability. The different alloys offer different properties which makes them suitable for use in different applications [45].

Figure 20 shows a 3D model of how the extruded T-track could look like. It is important to dimension it correctly. T-tracks would allow the bracket to slide right into the tracks and avoid any movement sideways. It would however require some kind of extra attachment to avoid any movement vertically.
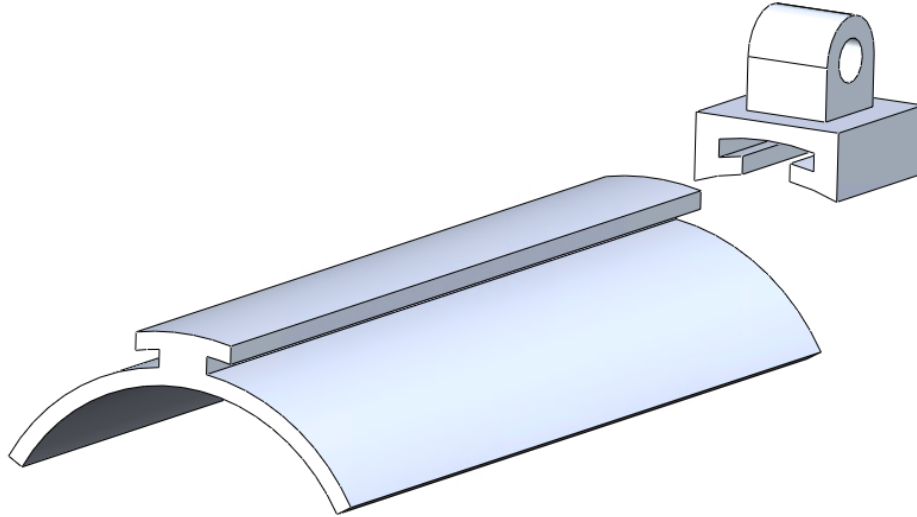
**Figure 20:** 3D model of the mast joined to the bracket using T-track connection

## 3.5. Choice of joining method

Based on a set-based approach and considering functionality, manufacturability and reliability, a combination of joining methods have been chosen. T-track as the main method, with bolt connections to prevent any movement in vertical direction. MIG-welding was eliminated mainly due to the lack of manufacturability and complexity, needing professionals and proper equipment. Bolt connections on its own was not chosen due to the low strength of aluminium bolts, and therefore uncertainty regarding reliability. By taking into account dynamic loads, the uncertainty will only increase due to wear.

There are several advantages of using T-track. The T-track offers excellent structural integrity due to its design characteristics. It provides a secure and robust connection between the mast and bracket, distributing the applied loads effectively. Extruded profiles offer high strength and rigidity, ensuring reliable performance. The manufacturing aspect of the T-track system is advantageous as well. Extrusion is a method that has high manufacturability, enabling modular construction and simplifying the supply chain processes. The addition of bolts will lower the manufacturability as well as the complexity, by having to precisely drill the holes in the correct position. It would however not require a lot of time and effort for installation. The joining method allows for easy disassembly and reassembly if necessary, providing convenient access for maintenance and repair activities. A downside with the joining method for this application is the material use. It would be necessary to have the T-track down the entire mast, which would result in high material use compared to the other methods.

Overall, extruded T-track offers high strength and material use, with a moderate complexity and manufacturability. It is important to note that the specific implementation of the T-track joining method will require further considerations and engineering analysis to ensure proper design, material compatibility, and appropriate load distribution. Additionally, any applicable codes, standards, and regulations should be followed during the design and implementation phases.

# 4. Simulation setup

This section will explain and present the simulation setup. This involves explaining the assumptions that has been made, as well as presenting values that will be used. World Wide Wind's choice of having the angle between mast and turbine blade at 55 degrees is mainly a design choice. Therefore, it will be looked into different angles, as well as different loads, for the joint. This to compare the results and how it affects the stress results. The model will be dimensioned with 6082-T6 to handle the 40kN load at 55 degrees with the applied safety factor. This model will then be used to obtain stress results for two other angles, 45 and 65 degrees, as well as two other loads, 50kN and 60kN. Finally, the stress results for the first model will be compared to three different alloys, 6005, 6061 and 6063, each with two different heat-treatments, T4 and T6.

## 4.1. Mechanical properties

The relevant mechanical properties to be able to perform the simulations and compare the stress results are the Young's modulus and yield strength. The yield strength for aluminium alloys can vary depending on various factors such as heat treatment, alloy composition, and manufacturing processes. Therefore, these values can vary. The values used in simulations and comparisons are shown in Table 1 and 2. The values for 6005-T4/T6 are found in [46, 47], 6061-T4/T6 in [48, 49], 6063-T4/T6 in [50, 51] and 6082-T4/T6 in [52, 53].

**Table 1:** Mechanical properties for different T4 aluminium alloys

|  | **6005-T4** | **6061-T4** | **6063-T4** | **6082-T4** |
|---|---|---|---|---|
| Young's modulus | 68 GPa | 69 GPa | 68 GPa | 69 GPa |
| Yield strength | 90 MPa | 110 MPa | 69 MPa | 110 MPa |

**Table 2:** Mechanical properties for different T6 aluminium alloys

|  | **6005-T6** | **6061-T6** | **6063-T6** | **6082-T6** |
|---|---|---|---|---|
| Young's modulus | 68 GPa | 69 GPa | 68 GPa | 69 GPa |
| Yield strength | 200 MPa | 241 MPa | 172 MPa | 240 MPa |

Determining the safety factor is not a simple and straightforward process for an offshore aluminium joint. The offshore wind turbine industry's inexperience in terms of its own regulations and standards is obvious as a direct result of the quick expansion and the rising demand for renewable energy production. The oil and gas industry originally provided these standards, keeping the corresponding reliability levels, safety considerations, and design techniques. However, as wind turbines are active devices rather than passive structures, these guidelines were not meant to apply to them. Additionally, from the perspective of structural design, there are a number of factors that are not present in their onshore counterparts. Such as the harsh salt water environment, the interaction and uncertainties in the various sources of loading. All of these must be taken into account in the design of offshore wind turbine support structures. Despite the long-term usage of these standards, it is generally acknowledged that the dependability levels attained are poorly understood, and the resulting partial safety factors may not be ideal for offshore wind turbines. A. Morato and S. Sriramula concluded in their study about calibration of safety factors for offshore wind turbine support structures that a safety factor of 1,35 would be enough for monopiles. Other cases could have a safety factor varying from 1,3-1,6 [54]. There is uncertainty about the safety factor that is needed. It depends on usage and standards, among other things. The safety factor at 1,3-1,6 will be rounded up to 2 and used further in these simulations.

## 4.2. 3D Modeling and geometry of components

World Wide Wind's turbine consists of two different size masts that rotates opposite direction with a rotary bearing in-between. The largest mast, with a diameter of 250 mm, will be used in the simulations. Only one third of the model will be modeled and simulating, utilizing the symmetry. The length of the mast is set at

500 mm even though the original mast is longer. This will not affect the stress results, just creating longer simulation time.

As in the bolt calculations, it was chosen to apply a total of four bolts. This is to better distribute the stress on the bolts. Even more bolts could be used to distribute the stress even more, but it is assumed that the bolts will not experience the highest stress. More holes can potentially reduce the materials strength and increase stresses. M15 bolts are used to handle the load as well as the stresses that appear around the holes. This is also the reason that the bolt spacing is larger than calculated. Rounded corners are also used to reduce local stress concentrations in corners and edges.

Figure 21 shows the 3D model of the extruded T-track design, Figure 22 shows the 3D model of the bracket design and Figure 23 shows the 3D model of the bolts. These components are put together in an assembly, applied mechanical properties, interactions, boundary conditions, loads, mesh and simulated. Mechanical drawings of the parts made in SOLIDWORKS and placed in the Appendix.
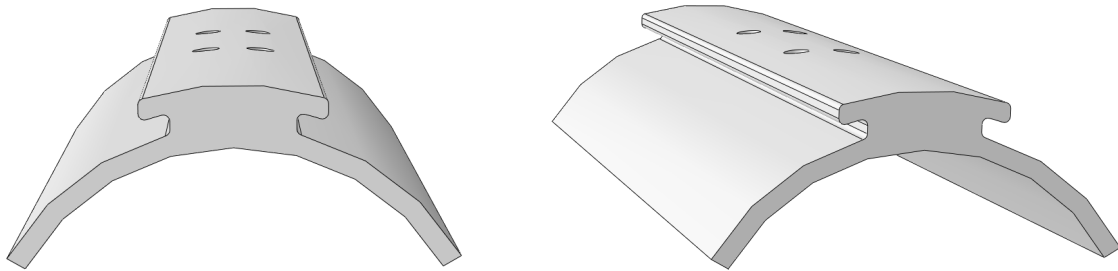


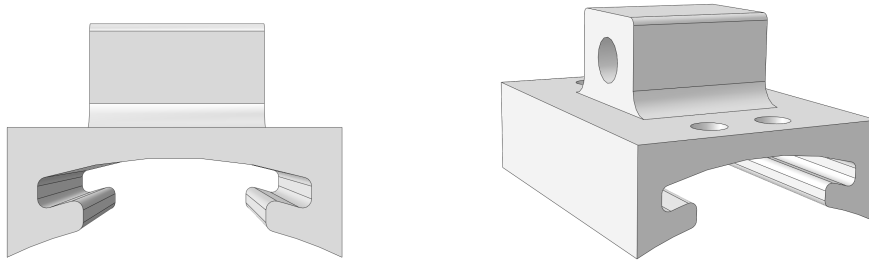**Figure 21:** 3D model of the extruded T-profile design



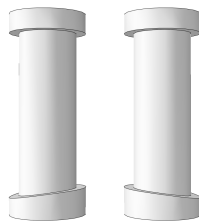**Figure 22:** 3D model of the bracket design



**Figure 23:** 3D model of the bolts

## 4.3. Boundary conditions

The boundary condition are placed on top and bottom of the mast, having it fixed in all directions. General contact set is created, to prevent the components penetrating. This is applied for the entire model. The horizontal force is placed on the right surface, while the vertical force is placed on the bottom surface. Since the goal is to dimension the T-track and bracket, the load is placed on the flat surfaces rather than in the hole. Placing the forces in the hole would result in the large stress concentrations in and around the hole. The entire model with applied boundary conditions and loads is shown in Figure 24.
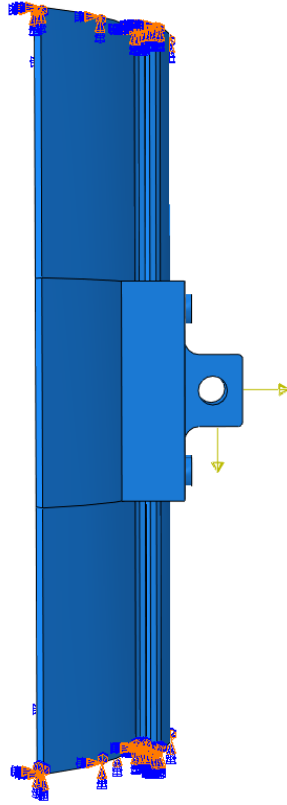
**Figure 24:** Configuration of fixtures and the applied load in the simulation

The coupling feature is used on the flat surfaces to create a relationship between the surfaces and the reference points as shown in Figure 25. Both the vertical and horizontal forces are placed in the reference points in the middle of the surface.
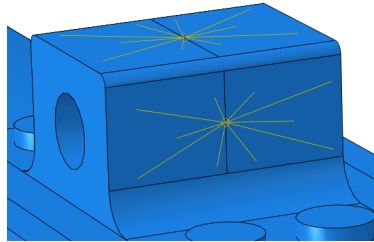


**Figure 25:** Coupling configuration

As mentioned, different cases of angles and loads will be looked into. Figure 26 shows the calculation result for the horizontal and vertical load that will be applied for the different angles and loads. For the different cases, it is assumed that the length between the blade joint and bracing joint is constant and that the bracing is connected in the middle of the blade. So when the angle of the blade changes, both the angle and length of the bracing also changes.

| | 40kN | | 50kN | | 60kN | |
|---|---|---|---|---|---|---|
| | Fx [N] | Fy [N] | Fx [N] | Fy [N] | Fx [N] | Fy [N] |
| **45°** | 38582,30 | 10554,92 | 48227,87 | 13193,65 | 57873,45 | 15832,38 |
| **55°** | 37087,35 | 14984,26 | 46359,19 | 18730,33 | 55631,03 | 22476,40 |
| **65°** | 35317,90 | 18778,86 | 44147,38 | 23473,58 | 52976,86 | 28168,29 |

**Figure 26:** Decomposed forces for 45, 55 and 65 degree angle with 40, 50 and 60kN load in [N]

## 4.4. Mesh

The Finite Element mesh (FE) of the model should be of high quality to get the most precise results as possible. The Finite Element Method (FEM) results may be less accurate, or in the worst case scenario, completely incorrect if a mesh of low quality is used. Each finite element is built to function correctly up to a specified level of element distortion before degenerating. The type of element and numerical method utilized inside the element formulation largely determine how much distortion is allowed before degeneration. Increasing the FE mesh density is the simplest technique to increase the accuracy of the solution, provided that the mesh is free of singularities. Smaller pieces are typically less prone to deviate from the correct shape, however even when mesh density is increased, there may still be cases where quality standards are broken. Increased FE mesh density will also lengthen the time it takes for your analysis to execute and use more memory on your computer [55].

A convergence analysis is run to find the mesh size and type where the stress results converges to a value as shown in Figure 27. By reducing the size even more after it converges, would only lead to longer simulation time and possibly higher stress results. The same global and local seed size was applied for the entire model, and then looked at how it affected the stress result for the different parts. Due to some variability in the results, only the values that exhibit proper convergence are presented.
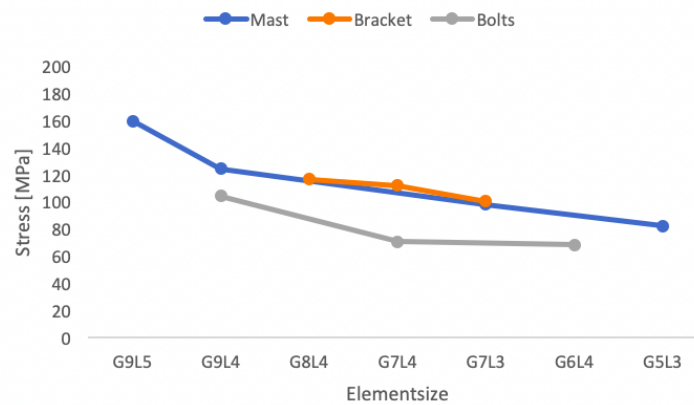


**Figure 27:** Convergence analysis of the three components

The convergence analysis resulted in a G5L3 for the mast, G7L3 for the bracket and G6 for the bolts. G represents Global seed size, indicating a size parameter that applies to the entire system. On the other hand, L represents Local seed size, referring to a size parameter specific to individual components or regions within the system. The local seeds are applied in the area where the high stress areas will occur. These being in the holes of the mast and bracket, as well as in the transition area of the bracket's protruding part. Hexagonal shape is the preferred element shape employed for both sweep and structured techniques. The mesh representation utilized in the simulations is illustrated in Figure 28.
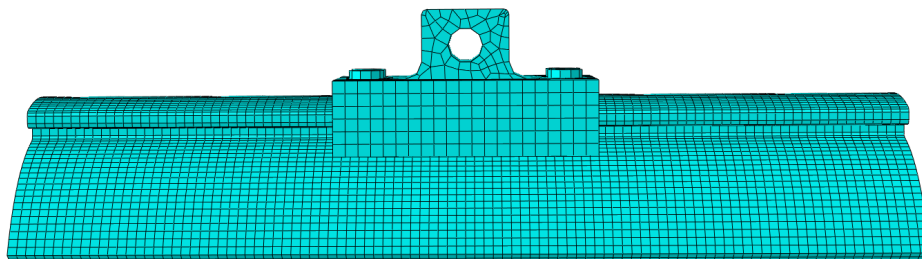


**Figure 28:** Mesh representation used in the simulation for accurate numerical analysis

# 5. Simulation results

## 5.1. Stress result for base model

Figure 29 illustrates the stress distribution across the entire model for World Wide Wind's standard, at a 55 degree angle and a 40 kN load. The maximum stress that occur in this structure is 101,4 MPa.
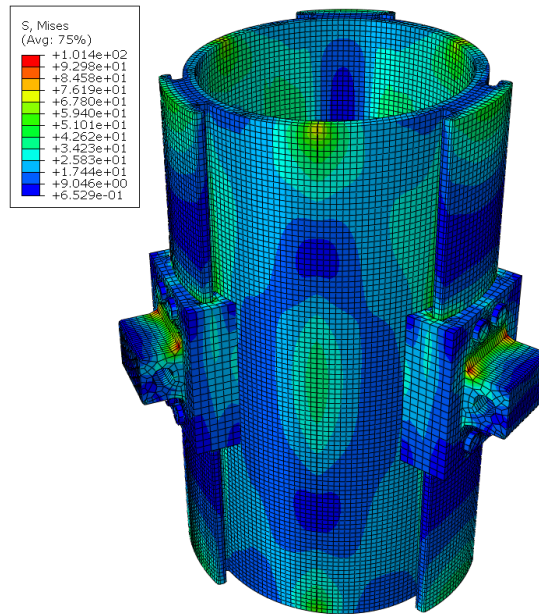


**Figure 29:** Overall stress distribution in the assembly at 55 degree angle and 40kN load

Figure 30 illustrates the stress distribution of the mast, at a 55 degree angle and a 40 kN load. The highest stress occur around the upper holes, with a value at 93,11 MPa.
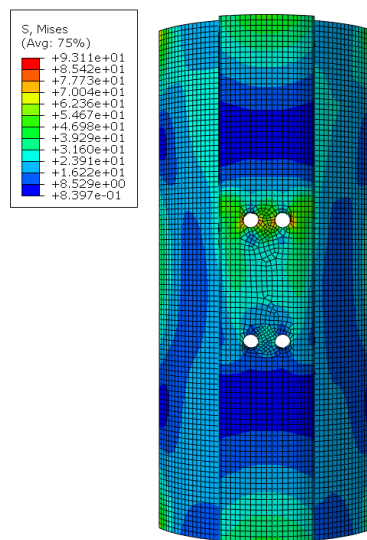


**Figure 30:** Stress distribution on the mast at 55 degree angle and 40kN load

Figure 31 illustrates the stress distribution of the bracket, at a 55 degree angle and a 40 kN load. The highest stress occur in the transition area of the bracket's protruding part, with a value at 101,4 MPa. This is the highest stress area of the entire assembly.
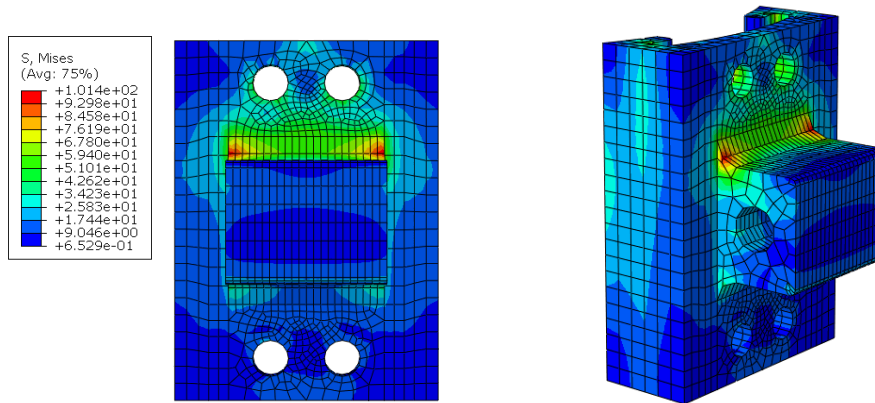


**Figure 31:** Stress distribution on the bracket at 55 degree angle and 40kN load

Figure 32 illustrates the stress distribution for both the upper and lower bolts. The upper bolts experience a stress of 72,32 MPa, while the lower bolts experience a stress of 26,53 MPa. For both the upper and lower bolts, the highest stress occur in the transition between bolt and head.
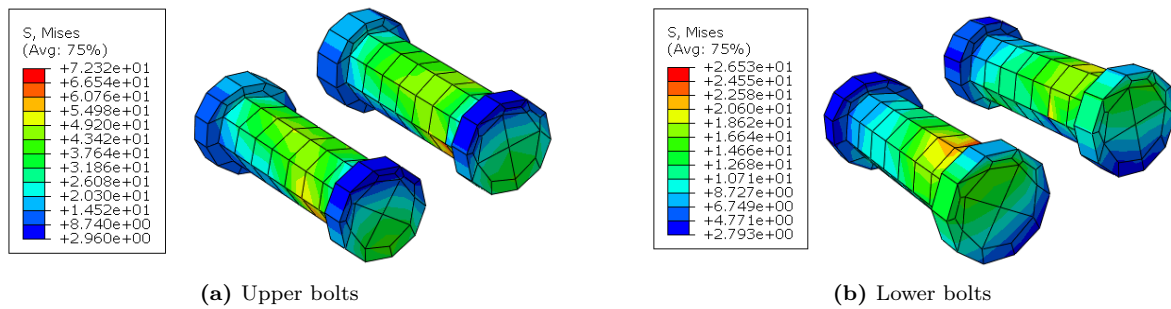


**(a)** Upper bolts

**(b)** Lower bolts

**Figure 32:** Stress distribution on the bolts at 55 degree angle and 40kN load

## 5.2. Stress result for 40kN load

Figure 33 illustrates the stress results for T-track assembly under a 40 kN load for angles of 45 and 65 degree. The stress values for these angles are 94,77 and 106,1 MPa, respectively.
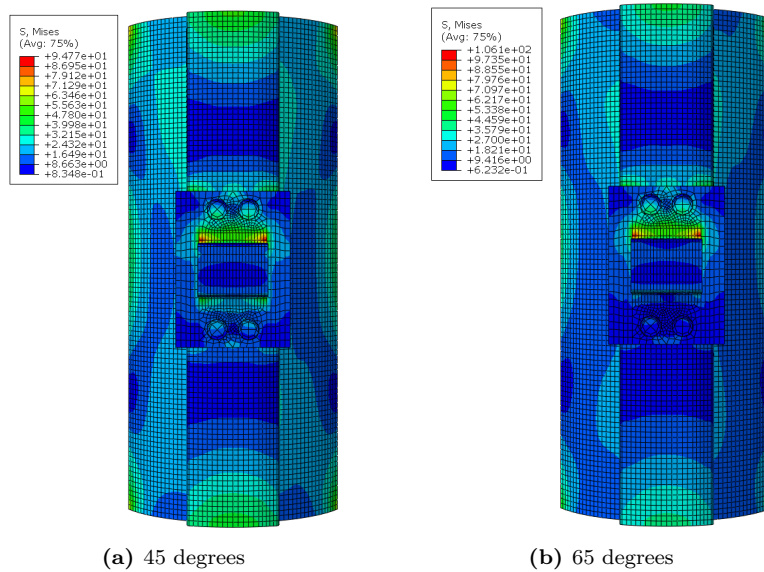


**(a)** 45 degrees        **(b)** 65 degrees

**Figure 33:** Stress distribution for assembly at 45 and 65 degree angle with 40kN load

## 5.3. Stress result for 50kN load

Figure 34 illustrates the stress results for T-track assembly under a 50kN load for angles of 45, 55 and 65 degree. The stress values for these angles are 118,3, 126,5 and 132,5 MPa, respectively.
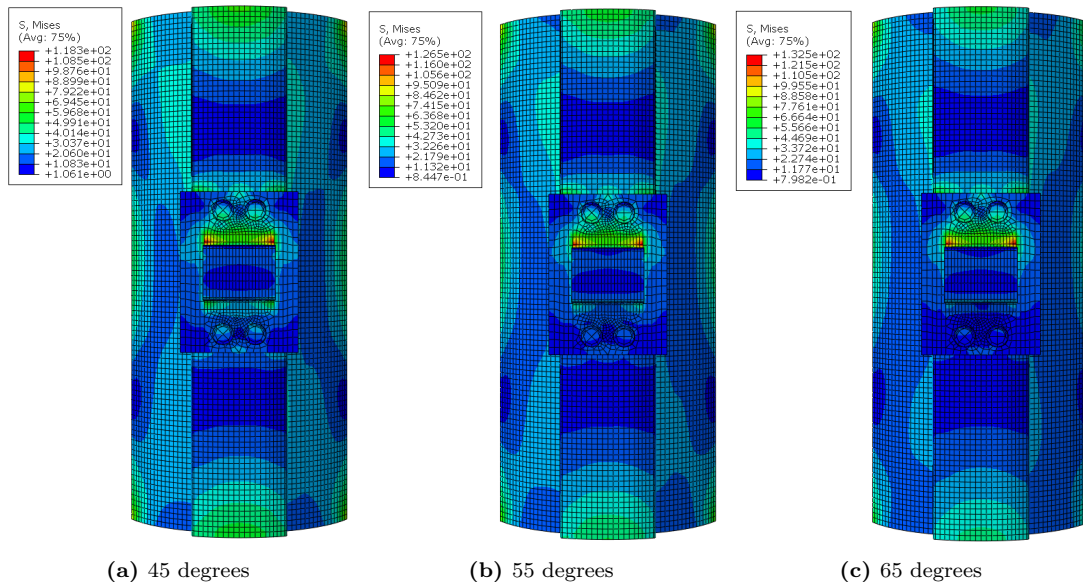


**(a)** 45 degrees      **(b)** 55 degrees      **(c)** 65 degrees

**Figure 34:** Stress distribution for assembly at 45, 55 and 65 degree angle with 50kN load

## 5.4. Stress result for 60kN load

Figure 35 illustrates the stress results for T-track assembly under a 60 kN load for angles of 45, 55 and 65 degree. The stress values for these angles are 141,8, 151,6 and 158,8 MPa, respectively.
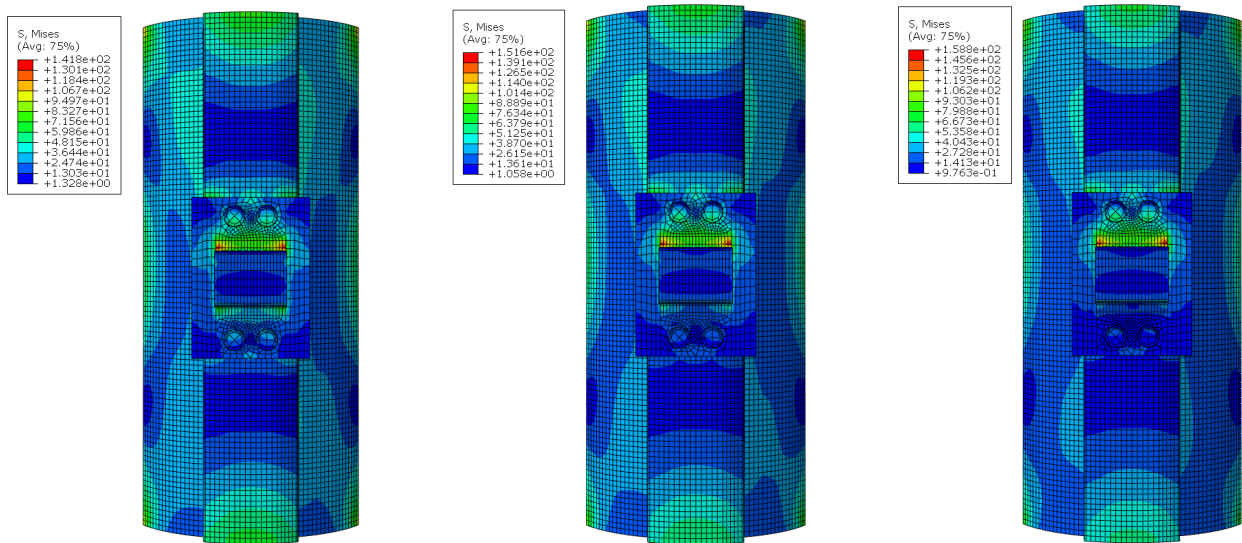


**Figure 35:** Stress distribution for assembly at 45, 55 and 65 degree angle with 60kN load

## 5.5. Comparison of stress results

In Figure 36, a Python-generated plot is presented, illustrating a comparison of stress levels across three different angles and three different loads. The dotted lines represent the yield strength and the yield strength with a safety factor of 2. All three cases with a 40 kN load as well as 40 kN load at 55 degree fall within the safety factor of 2. All the other cases have stress levels that exceeds the safety factor.
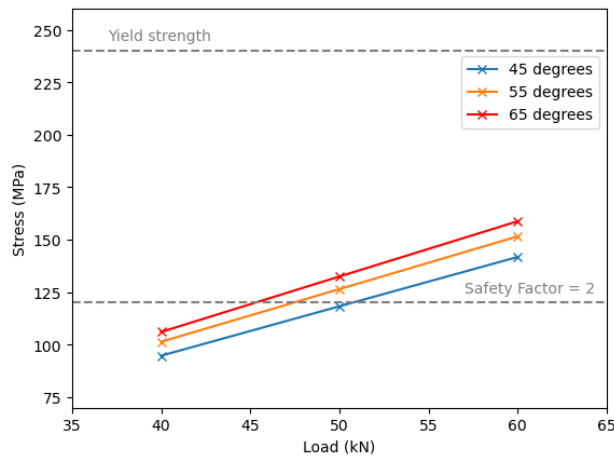


**Figure 36:** Comparison of stress results for different loads and angles

## 5.6. Stress results for different aluminium alloys

In Figure 37, a Python-generated plot is presented. The figure illustrates a comparison of experienced stress levels at a 55 degree angle and 40 kN load with yield strength for different aluminium alloys. The dotted line visualizes the experienced stress at 101,4 MPa.
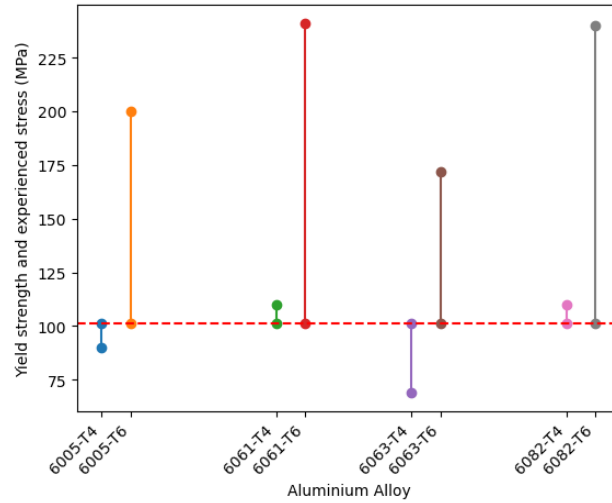


**Figure 37:** Comparison of yield strength and experienced stress for different alloys at 55 degrees and 40kN load

# 6. Discussion - joining method

The first objective of the master's thesis is to investigate the possibility of combining offshore wind turbines with aluminium components and to establish a reliable connection between the mast and turbine blade. The focus is mainly on functionality, manufacturability and reliability of the joint. To achieve this objective, the thesis considers multiple scenarios and criteria, and evaluates two major joining techniques; standard component that is MIG-welded or using bolt connection and special purpose extrusion T-track design.

MIG welding is known for its strength in joining aluminium components. The welding process will however reduce the strength in the HAZ. This can lead to additional material being necessary to counteract. The calculations showed a minimal reduction in characteristic strength for weld at 190 $N/mm^2$ to HAZ at 185 $N/mm^2$. A different filler material could result in a higher characteristic strength and should therefore be carefully considered. The filler metal that is necessary for MIG-welding also adds to the material use in the form of a wire. Additional material to the joint will increase the weight and material consumption, but compared to the other two joining methods the material use is low. MIG welding offers the advantage of versatility, as it can be used with various aluminium alloys. Complexity-wise, MIG welding can be moderately complex. It requires skilled welders who are experienced in welding aluminium and proper equipment to ensure a successful weld. Additionally, the need for surface preparation, shielding gas, and filler material adds to the complexity of the process. These will require careful control of gas flow rates and wire feed. MIG welding have some challenges in terms of manufacturability, that results in the method having low manufacturability. The welding itself is a process that is not easily manufacturable. In addition, the welding process also involves proper surface preparation, such as cleaning and removing oxide layers, which adds to the manufacturing steps.

Bolt connections are widely employed as a joining method and offer a straightforward approach for connecting aluminium components. The strength of the connection primarily depends on the bolt material and the clamping force applied during assembly. When properly designed and tightened, bolt connections can achieve high strength and stability. Aluminium bolts that are used in the calculations have a significant lower strength at 315 MPa than steel bolts at 800 MPa which are more commonly used. Due to the leap in strength, bolt connections alone created uncertainties regarding the reliability. In terms of material use, bolt connections typically don't require much additional material. A bit of additional material is needed due to requirements of distance between bolts and edges. Bolt connections are considered low complexity and high manufacturable. The process involves drilling holes with automated equipment, aligning the components and tightening the bolts with standard tools. Assembly and disassembly can be relatively straightforward, making bolt connections a preferred choice in situations where maintenance or replacement of components is necessary. The use of standard bolts and nuts simplifies the sourcing and availability of the necessary fasteners.

The extruded T-track with bolt connection combines the advantages of extruded aluminium profiles and bolt connections. In terms of strength, the extruded T-track with bolt connection can offer high strength, especially when designed appropriately and considering factors such as track dimensions and material selection. The T-track design allows for distributing the load and increasing the stiffness of the joint. Material use in the extruded T-track with bolt connection can however be relatively high compared to the other methods. It will lead to high material use with having the T-track down the entire mast. The T-track, when extruded and combined with bolt connections, possesses a moderate level of manufacturability. While the individual joining methods exhibit high manufacturability on their own, their combination necessitates additional work and reduces overall manufacturability. As a result, the complexity will be increased. The extrusion process itself requires specialized equipment and expertise, but once the profiles are manufactured and the holes are drilled, the assembly process becomes relatively straightforward. A moderate complexity can be assumed. The extruded T-track provides a structural framework, simplifying the alignment of components during assembly. The complexity can thus vary depending on the specific design and tolerances required.

Table 3 shows a comparison for the three joining methods with regard to strength, material use and complexity.

**Table 3:** Comparison of joining techniques

|  | Strength | Material use | Complexity | Manufacturability |
|---|---|---|---|---|
| MIG welding | Moderate | Low | Moderate | Low |
| Bolt connection | Moderate | Low | Low | High |
| T-track with bolt connection | High | High | Moderate | Moderate |

Upon analysing the various scenarios considering different loads and angles, it was observed that lower angles corresponded to lower levels of stress, as expected. Only four cases were within the safety factor of 2 ensuring the joint's strength and reliability; the three cases with a 40 kN load and the 45 degree with 50 kN load. For the other cases, modifications should be made to meet the requirements. However, it is crucial to acknowledge the uncertainty surrounding the safety factor. The safety factor was selected to provide a substantial margin of safety. For a more precise determination of the safety factor, further research is necessary. A more accurate safety factor will result in a more precise model.

The permissible stress plays a significant role in determining the load capacity of a material. Different alloys exhibit varying yield strengths, as demonstrated in the comparison of experienced stress and yield strength among different alloys. Changes in Young's modulus have minimal impact on the stress results. However, the yield strength differs significantly among alloys, leading to variations in the allowable stress. The comparison was performed using the model dimensioned for a 55 degree angle and 40 kN load. Among the four alloys examined, the T6 alloys exhibit higher strength than the T4 alloys. The yield strength of T4 alloys is either slightly above or below the experienced stress levels. In contrast, all T6 alloys have a yield strength well above the experienced stress, providing a comfortable margin of safety. This comparison underscores the importance of selecting the appropriate alloy for a specific application, considering not only strength but also other relevant properties.

It is crucial to acknowledge that the calculations and simulations performed in this thesis focus exclusively on static loads and do not incorporate dynamic loads and fatigue life. Both of which can have a substantial impact on the long-term performance of the joint. While the examination of static loads provides a starting point for analysing and exploring the joining methods, it is important to recognize that a comprehensive assessment necessitates inclusion of dynamic loads and fatigue life. Incorporating dynamic loads and fatigue life into the analysis will provide more precise and reliable results, enabling a deeper understanding of the joint's behavior and performance in real-world scenarios.

In summary, the various joining methods offer different properties that make them viable options. T-track, for instance, provides higher strength but requires more material usage. On the other hand, MIG-welding offers low material consumption but limited manufacturability. Bolt connections, however, possess the advantage of good manufacturability while providing moderate strength. To determine the best option, further research and testing are recommended. By conducting additional investigations, it will be possible to evaluate the joining methods more comprehensively and identify the most suitable approach for the specific requirements.

# 7. Cost and environmental impact of aluminium production and transportation

Extrusion offers several advantages such as high production speed, material efficiency, and design flexibility. In terms of cost, extrusion can be cost-effective for producing long and continuous profiles. It minimizes material waste since the desired shape can be achieved with minimal machining or additional processing. As for emissions, extrusion typically requires significant energy input for heating and forcing the material through the die. However, if the extruded profiles require little post-processing and machining, the overall emissions can be lower compared to other methods. Having selected T-track as the joining method, the attention is now turned to the manufacturing and logistics of the assembly. The major part of cost and emissions for an aluminium product comes from production and shipping. This part of the thesis will look into different cases of production lines for aluminium. Production lines with differences in primary/post-consumer aluminium, energy source and transportation length will be presented. The results will give an indicator on the differences and the way going forward. First, some vital information will be presented with regard to production, emission and cost.

## 7.1. Aluminium production

The primary component used in manufacturing of aluminium is bauxite. This is a soil resembling clay type that is found in a strip around equator. The extraction of bauxite involves digging a few meters beneath the surface to access the bauxite deposits. The extracted bauxite is then transported to processing facilities, where the clay is separated and the bauxite is subjected to grinding. Through this refining process, alumina is obtained. The extraction of alumina is carried out by using a heated mixture of caustic soda and lime. This process separates the alumina from the bauxite, and the remaining alumina is dried to form a white powder through heating and filtration. Once the alumina has been refined, it is sent to a metal plant where the production of aluminium takes place. The production of aluminium involves the use of three primary materials: carbon, electricity, and aluminium oxide. In the production process, a carbon-based negative cathode and a positive anode are used to conduct electricity. The oxygen present in the alumina reacts with the carbon anode, resulting in the production of carbon dioxide $CO_2$. As a result, the cells contain liquid aluminium that can be tapped. Depending on its intended use, the liquid aluminium is cast into various forms such as extrusion ingots, sheet ingots, primary foundry alloys, or wire rods. The aluminium can be further processed through extrusion, rolling, or remelting to produce a wide range of aluminium products [56]. This process is shown in Figure 38.
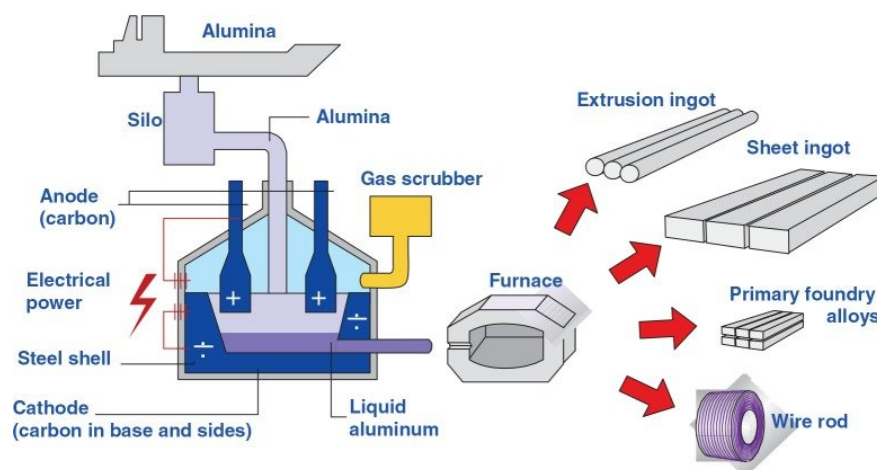


**Figure 38:** Aluminium production [57]

## 7.2. Emission

As of 2011, transport of goods and people accounted for 20% of all GreenHouse Gas emissions (GHG) in the EU, a percentage that has been steadily rising over the years since then. Around one-third of all transport-related GHG emissions come from the transportation of freight. Industry has already made significant efforts to increase the energy efficiency of freight transportation. However, there has been a significant rise in global trade and the further integration of the expanded EU. These increases in energy efficiency have not been enough to offset the growth in emissions produced by higher transport freight quantities. Europe is on a responsible route to achieving climate neutral by 2050 thanks to the Commission's proposal to reduce greenhouse gas emissions by at least 55% by 2030. Reduction of transport-related $CO_2$ emissions could be a significant contributor to this [58, 59]. New and more environmentally friendly ways of shipping are constantly being researched. Hydro is investigating the possibility of using block trains as well as ships with rotor sails to reduce fuel consumption [60].

Russia's invasion of Ukraine has resulted in rising energy prices, and reduced producer profits with metals having a high energy content being particularly impacted. Shutdown of aluminium smelters occurs as Europe works to increase its level of independence in the wake of Russia's conflict in Ukraine. The region becomes more dependent on more expensive imports from sources with higher carbon emissions, such as China, as more smelters close. Smelters in Europe produce three times less carbon dioxide than those in China, where coal is most frequently used to produce energy [61].

Figure 39 shows the differences in carbon footprints in terms of where it is produced and used. The main difference lies in the energy source utilized. The three relevant poles for the this study are Hydro CIRCAL 75R (minimum 75% recycled aluminium), primary aluminium produced by Europe and primary aluminium produced in China.
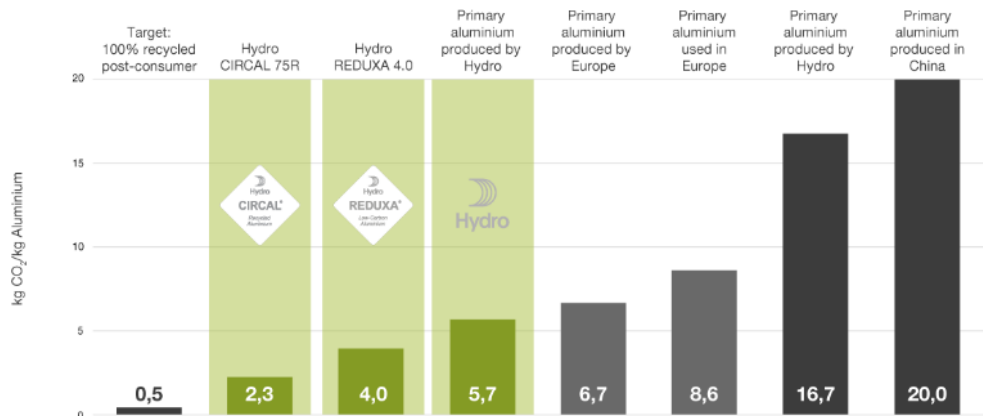


**Figure 39:** Comparison of carbon footprint for production and use in different locations [62]

## 7.3. Cost

When examining the price of aluminium, it is clear that volatility is is present to the highest degree. The aluminium market relies on the London Metal Exchange (LME) as a benchmark for pricing. The LME is the world's premier non-ferrous metals market, facilitating the trading of metals including aluminium. However, China, as a significant player, also operates its own aluminium pricing system known as the ShangHai Futures Exchange (SHFE). SHFE is also a market for aluminium. Both LME and SHFE works in the same way with regard to trading of aluminium, but they operate independently. The SHFE price can fluctuate, sometimes surpassing the LME price and other times falling below it. The price of post-consumer scrap aluminium is based on the LME, but typically lower. The purity of the scrap also influences its price, with higher purity levels commanding higher values. Furthermore, there exists a premium factor that can impact the price. Producers may receive a premium for low emissions in production or the inclusion of post-consumer scrap. However, accurately quantifying the value of such premiums in the market remains a challenge [63].

In the case of companies like Hydro, standardized prices are agreed upon for transportation routes, with the only variable being a fuel clause [60]. These agreements are typically based on typical shipments, with various factors that influence the final price. The distance traveled plays a significant role, as longer distances generally incur higher costs. However, there are limits to how far shipments can reach, taking into account logistical constraints, start-up costs, and the consideration of return shipping [63]. Arrangements are often made to avoid empty return trips, ensuring that ships or trucks have a full load for the return journey. The fuel clause, on the other hand, varies depending on the prevailing fuel prices. The purpose of such agreements is to ensure cost predictability and stability, minimizing unexpected variations. For ocean freight are rates affected by the size of the vessel and the market dynamics, which can be relatively volatile. As a result, even for the same route and load, the price of shipping can fluctuate significantly, ranging from \$2500 to \$20000 [60].

### 7.3.1. Carbon tax

To reach the goal of reducing carbon emissions, many different forms of carbon taxes exists. There is a possibility of so-called carbon leakage when the EU increases its own climate ambition and as long as less strict climate policies are common in many non-EU nations. When businesses located in the EU relocate carbon-intensive production to nations with poorly enforced climate regulations than the EU, or when EU products are replaced by more carbon-intensive imports, carbon leakage occurs. The Carbon Border Adjustment Mechanism (CBAM) of the EU is our ground-breaking tool for pricing carbon emissions from the production of commodities entering the EU fairly and for promoting cleaner industrial production in non-EU nations [64].

Despite being the EU's largest trading partner, China's exports to the EU won't be significantly impacted by CBAM in its current form, according to a number of analysts. Nonetheless, they anticipate that it will serve as a external incentive for China's national Emissions Trading System (ETS) to expand in order to balance off certain long-term effects. Manufacturers outside the EU will only be required to declare their emissions during a transitional period from October 2023 to December 2025. Following that, a charge will gradually be implemented from 2026 to 2034, requiring EU importers to buy certificates equal to the weekly EU carbon price [65]. The EU ETS are working on a principle called the cap and trade. The overall amount of particular greenhouse gases that the operators covered by the system may emit is limited. Over time, the cap is lowered to reduce overall emissions. Operators purchase or receive emissions allowances within the cap, which they can exchange with one another as necessary. The restriction on the overall amount of available allowances makes sure that they have a purpose. While trading gives flexibility that ensures emissions are reduced where it is least expensive to do so, the price signal encourages emission reductions and encourages investment in cutting-edge, low-carbon technologies. An operator must surrender enough credits each year to adequately cover its emissions or face large fines. By reducing its emissions, it is possible to sell to someone short of allowances or keep the spare allowances to cover possible future needs [66].

As explained in this subsection, the carbon tax is a complex policy instrument due to its numerous variables and the volatile nature of the market it operates within. The variables involved, such as the carbon price, emission sources, tax rate structure, tax base, revenue allocation, and compliance mechanisms, introduce a level of intricacy that requires careful consideration during the design and implementation phases. Moreover, the carbon market itself is subject to fluctuations influenced by factors like economic conditions, political dynamics, and international agreements. These complexities and market volatility can make it challenging to accurately predict the outcomes and impacts of a carbon tax. Consequently, the focus of the thesis is on the overall picture of production and shipping, and the inherent complexity of the carbon tax is therefore overlooked. For a more precise result, the carbon tax is an important factor and should be included in the calculation.

# 8. Production lines

In this study, three different cases will be compared to analyse their respective implications. The first case represents the longest production line all the way from China to Europe, and the second case has a production line from Slovenia to Norway. The third case explores an integrated production process that utilizes post-consumer metal, with all manufacturing stages taking place under the same roof. The production line in the cases are only hypothetical to highlight differences in cost and emission.

To establish a consistent comparison, Stavanger is chosen as the final location for all three cases. This selection is primarily motivated by its coastal position, which offers convenient access to docks. Furthermore, Stavanger is located just a few hours drive away from Karmøy, where a Hydro facility with a smelter is situated. In terms of price and emissions calculations, certain assumptions need to be made. Three different production volumes is assumed; 25, 20 000 and 100 000 tonnes. This will give an indicator of how production volume can affect the cost and emission per tonne aluminium produced.

To facilitate emissions comparison, a container ship is employed as a reference for ocean shipping since it allows for easier emissions comparison and can be applicable to transportation via truck as well. It should be noted that emissions can vary depending on the specific transportation method and the type of ship utilized.

Figure 40 presents a map illustrating the distribution of offshore wind turbines in Norway. The wind turbines are primarily concentrated along the coastline, with a few located offshore from Stavanger. This geographical distribution further justifies the selection of Stavanger as the final location.
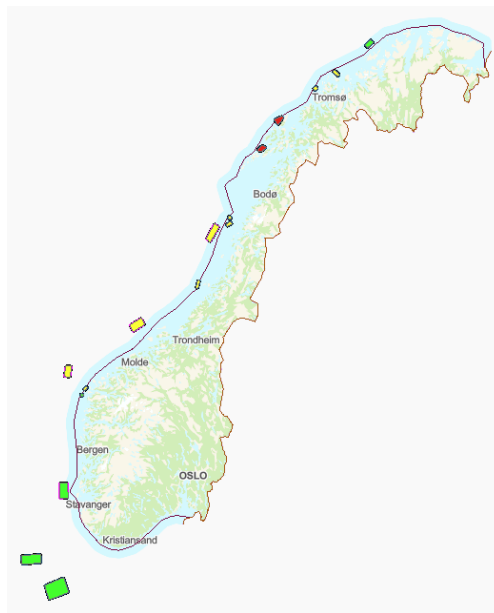


**Figure 40:** Distribution of wind turbine farms across Norway [67]

The wind farms pictured on the map are distinguished by three distinct colors, each corresponding to different categories: A, B, and C. The color green represents category A, which signifies areas that have been specifically designated and reserved for offshore wind energy development. These areas have undergone initial planning and evaluation, indicating their potential suitability for establishing wind farms. Category B, represented by the color yellow, encompasses areas where detailed assessments, comprehensive studies, and thorough evaluations have been conducted. The yellow color indicates that these areas have progressed beyond the initial planning stage and are in a more advanced phase of development. The color red designates category C, which comprises areas where wind turbine farms are already operational or currently under construction. The red color signifies that these areas represent the most advanced stage of development, with wind farms that are actively producing energy or in the process of being constructed [67].

For emissions calculations, a value of 62 g $CO_2$/tonne-km will be used for trucks, while 13,5 g $CO_2$/tonne-km will be used for ships [58]. It is a bit more difficult to calculate the freight cost, since there usually is an

agreed price, and not a price rate that is based on distance and load. However, based on research, a rate has been made which results in reasonable prices for the various shipping routes. These are respectively 1 NOK/tonne-km for truck and 0,05 NOK/tonne-km for ship [63].

## 8.1. Case 1

China is a big producer of primary aluminium. They are also the world's third largest producer of bauxite as of 2022 after Australia and Republic of Guinea [68]. It is therefore not necessary for them to import bauxite. Primary aluminium requires a lot of energy to be produced, and leave a big carbon footprint. The carbon footprint is even higher in China, due to the fact that they use fossil fuel in the form of coal as energy source. Fossil fuel are made from decaying plants and animals as the components. These fuels may be burned to provide energy and can be found in the crust of the Earth. An example of a fossil fuel is coal, as well as oil and natural gas. It is unfortunate that fossil fuels are a finite resource, and it is impractical to wait millions of years for new coal, oil, and natural gas deposits to emerge. Additionally, nearly three-fourths of the emissions from human activity over the past 20 years can be attributed to fossil fuels [69] In 2022, 63% of China's electricity generation was from coal, and is by far the largest proportion [70]. Primary aluminium produced in China, by coal, produces a carbon footprint of 20 kg $CO_2$ per kg aluminium [62].

The primary aluminium will be produced in a factory in China. After the production, the aluminium is shipped by ship from Shanghai to port of Amsterdam in the Netherlands. The freight is then transshipped onto a truck and driven to Harderwijk. Here it is processed, before transported back to the port of Amsterdam. Once again, it is transshipped, before shipped to port of Norrkopping in Sweden. For a third time, the freight is transshipped. From Norrkopping, it is transported by truck to Finspång. There is a Hydro facility located in Finspång, with innovation & technology as well as extrusion. Once again, it goes through a processing process. Finally, it is transported to Stavanger in Norway by truck. The production line for Case 1 in Figure 41 shows the transportation route, a total of 22 177 km transport including three transshipments, and the production of the primary aluminium is by fossil fuel.
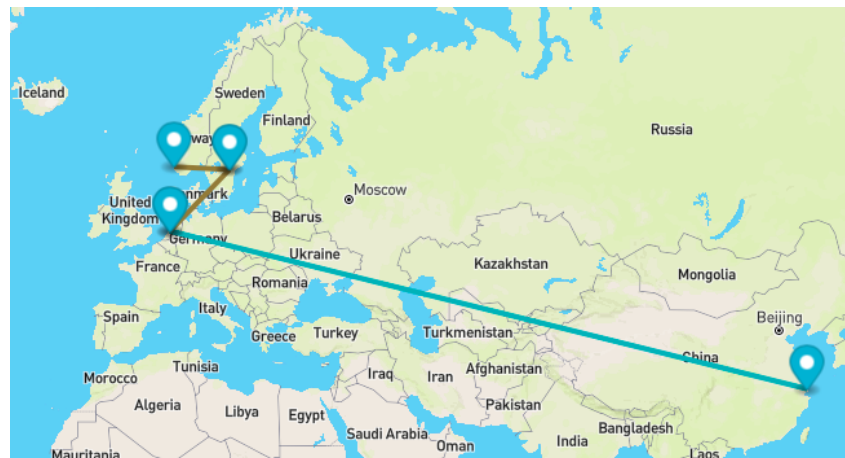


**Figure 41:** Production line - Case 1 [71]

The price of primary aluminium from China or East-Europe can be influenced by a range of factors including supply and demand, global economic conditions, and production costs. It is also worth noting that the price on aluminium can vary depending on the grade and form of the aluminium. For a simple analysis, one can assume that the aluminium price is similar whether it is produced in China or East-Europe. In 2022, the average price of aluminium was between $2 000-$4 000 per tonne. Using the average value of $3 000 per tonne with a currency rate on 10,6 results in the price being 31 800 NOK per tonne of primary aluminium [63].

## 8.2. Case 2

Unfortunately, because of rising electricity prices, many aluminium smelters in Western Europe have stopped manufacturing. Primary aluminium production in Western Europe dropped by roughly 12.6% and stood at about 2.9 MT in 2022. Talum located in Kidričevo is the largest manufacturer in Slovenia, lowered its output by 80% in 2022 due to high electricity prices. After nearly 60 years of producing primary aluminium, the Slovenian aluminium manufacturer Talum will stop using its last aluminium electrolytic furnaces in April 2023 [72]. However, Slovenia is still used as producer of primary aluminium in this case. Slovenia's electricity generation by nuclear energy was 38,58% from 2021-2022, being the second largest proportion after fossil fuel [73]. Nuclear energy is refereed to the energy inside the core of the atom. Nuclear reactors are collection of devices that is able to manage nuclear fission to generate electricity. Uranium atoms are split apart under extreme pressure in nuclear reactors. The atoms split, releasing little particles known as fission products. Other uranium atoms break as a result of fission products, beginning a chain reaction. This chain reaction releases energy, which is converted into heat. The heat warms the cooling agent in the reactor, which is typically water but might also be liquid metal or molten salt. During cooling, steam is produced. The steam rotates turbines or wheels that drives generators which produces energy [74]. Primary aluminium produced in Slovenia, produces a carbon footprint of 6,7 kg $CO_2$ per kg aluminium [62].

Slovenia do not produce their own bauxite and imports most of it from Brazil or India [75]. For every tonne of aluminium, 2 tonnes of alumina is used which again corresponds to about 4-5 tonnes of bauxite [76]. The required amount of bauxite is set at four times the desired production volume. This bauxite will be transported from the largest port in Brazil, port of Santos to the factory in Slovenia. The primary aluminium that is produced is transported to the dock in Koper by truck. The freight is transshipped to ship and transported to the port of Norrkopping in Sweden. It is once again transhipped, this time onto a truck and transported to Finspång. The metal goes trough a processing process before transported by truck to Stavanger in Norway. Figure 42 shows the production line for Case 2, a total of 8 443 km transport including two transshipments, and the production of primary metal is by nuclear power. In addition to the production line, is the import of bauxite from Brazil.
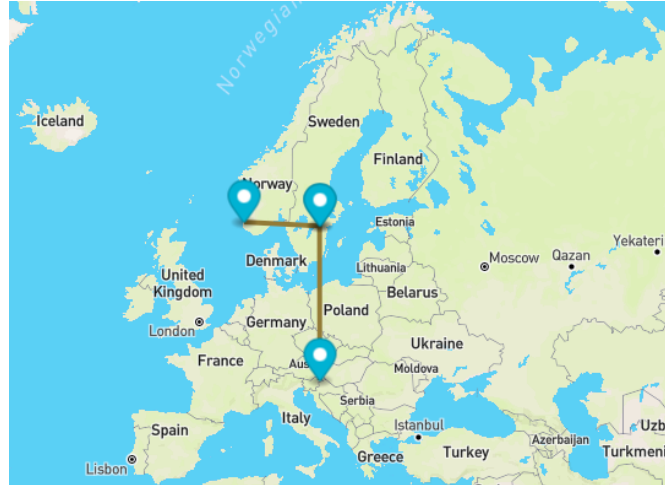


**Figure 42:** Production line - Case 2 [71]

The same price as in Case 1 will be used for the primary aluminium, at \$3 000 per tonne. With the currency being 10,6 will this result in a price of 31 800 NOK/tonne of primary aluminium [63].

## 8.3. Case 3

Norway is another country that produces a lot of aluminium, with Hydro as the biggest producer. The majority of Norway's electricity generation is from hydropower. In 2021, hydropower generated 90% of the total energy production in the country [77]. The majority of hydropower plants feature a mechanism for controlling the amount of water flow, frequently in the form of a reservoir, as well as an outlet or destination for the water after it flows downstream. Just before water rushes over the top of a dam or runs down a hill, it gains potential energy. Water flowing downhill changes potential energy into kinetic energy. Water is utilized to drive a turbine by rotating the blades, which powers a generator, which generates energy. Hydropower accounts for over 71 percent of all renewable electricity produced on Earth [78]. Primary aluminium produced in Norway, by renewable energy sources, produces a carbon footprint of 4,0 kg $CO_2$ per kg aluminium. Using post-consumer in form of Hydro CIRCAL 75R, the number is even lower at 2,3 kg $CO_2$ per kg aluminium [62]. Hydro CIRCAL 75R is certified to contain at least 75% scrap aluminium, with the rest being process scrap and primary aluminium [79].

For the integrated production process, post-consumer aluminium in the form of HYDRO CIRCAL 75R, will be gathered from five cities in Norway and transported to Stavanger by truck. Here it will be remelted by using hydropower. This case would however require constructing a factory for the production process.

When selecting the five cities that are used in the calculation of shipping cost and emissions, a population density map of Norway is used as shown in Figure 43. The red areas are the most populated ares with the yellow being the least. By looking at the map, it is clear to see that Norway's inhabitants are mainly to be found around Oslo or along the coast in the south and west. Five cities are used in the calculations to represent where people live. These cities are Bergen, Fredrikstad, Oslo, Tromsø and Trondheim. They are some of the largest cities in Norway, and thus also many residents. By spreading the five cities, it would be possible to gather post-consumer metal over large parts of Norway.
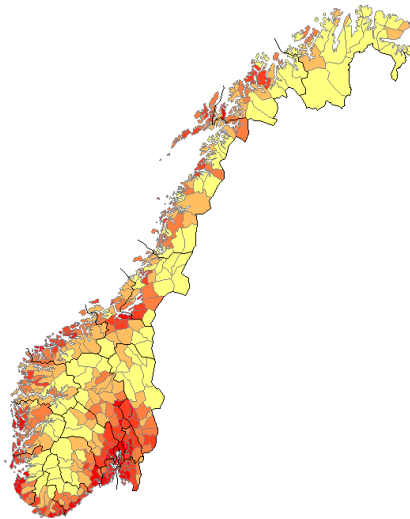


**Figure 43:** Population density map of Norway [80]

Figure 44 shows the different transportation routes. Five different routes will be used, each carrying a fifth of the production volume. The routes result in a total of 4 595 km transport separate, but some of the routes are possible to combine with a little detour. However, five separate routes and trucks will be used in the calculations. Since the cost of shipments usually are based on full loads, it would not be much cheaper for half a container compared to a full. Therefore the cost rate for truck for this specific case is set at five times more expensive than the other cases.
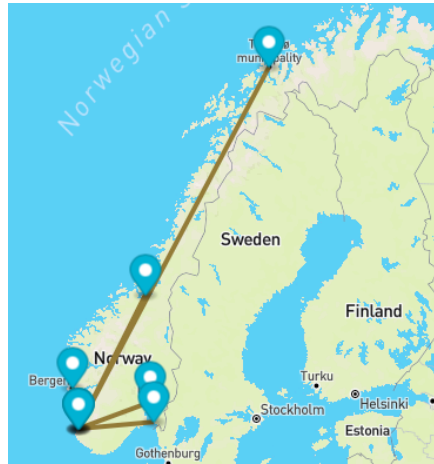
**Figure 44:** Transportation route - Case 3 [71]

The price of post-consumer aluminium remelted in Norway can vary depending on a range of factors such as the quality of the scrap, the cost of energy and raw materials, and market demand. Low grade scrap might sell for 60-70% of primary metal, with a higher quality scarp that even could be at 80-90%. While other types of scrap could be more in the vicinity of 30-40%. There is also more metal loss by using scrap, which can be considered a cost. But with a developing market, and with the advantage in emission that scrap holds, it could be more expensive in the future [63]. Assuming value of 40% cheaper than primary aluminium means the cost would be $1 800 per tonne resulting in 19 080 NOK/tonne post-consumer aluminium.

As mentioned earlier would this case require to construct a building. The building would house processes such storage, extrusion, cutting, Friction Stir Welding (FSW) and assembly as shown in Figure 45. There would be significant cost and emissions of construction the building. There is no need for the factory to house a remelter. It is assumed that there is an aluminium factory in the vicinity for remelting of the post-consumer metal and billet extrusion. With regard to the cost of the equipment necessary, these have been chosen to overlook. This is due to the fact that there are many unknown factors and it would result in a very complex calculations. The equipment size and capacity, production quantity and specifications are some of the factors that are unknown. Additionally, the investment for these types of equipment can be based on annual depreciation. A total of 17 000 $m^2$ is assumed required to house all processes under one roof. According to ByggFakta, the constructing cost for a retail floor area in Norway is approximately 10 500 NOK/$m^2$ [81]. This corresponds to 178,5 million NOK. The required area is only an approximate estimate, it is not an exact figure.
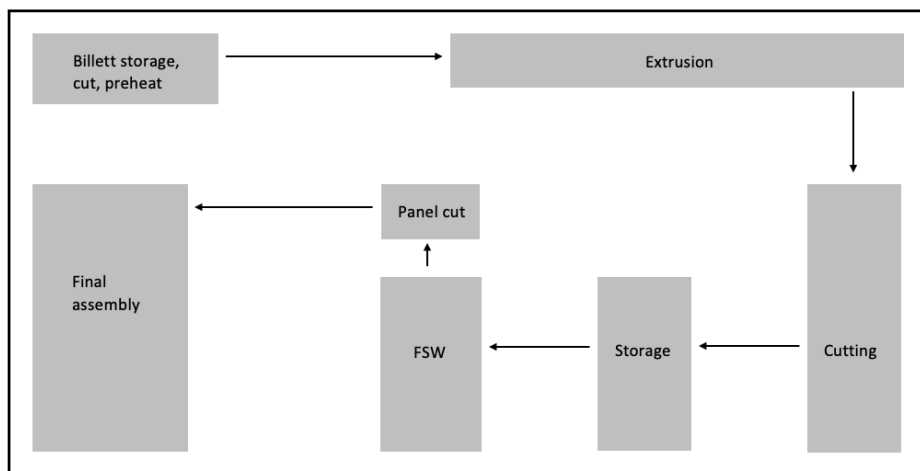


**Figure 45:** Warehouse

The amount of $CO_2$ emissions generated during the construction of a building can vary significantly depending on several factors, including the size of the building, the construction materials used, the construction techniques employed, and the energy sources utilized during construction activities. It is important to consider both direct and indirect emissions associated with construction. Direct emissions primarily arise from on-site activities such as energy consumption for construction machinery, equipment, and heating, as well as from the burning of fossil fuels during transportation of materials and waste management. These emissions can be estimated by considering the fuel consumption rates and emission factors for the machinery and vehicles used. Indirect emissions are associated with the production, transportation, and disposal of construction materials. These emissions are attributed to processes that occur outside the construction site, including the extraction and manufacturing of raw materials, transportation of construction materials to the site, and waste generated during construction [82]. The emissions associated with these activities can be estimated using Life Cycle Assessment (LCA) methodologies, which take into account the energy consumption and emissions associated with each stage of a material's life cycle. However, this would require a lot of work and time, and for that reason will a rough estimate based on size will be used. Silvia Dimova stated in here study about environmental benchmarks for buildings that it was not possible to establish a trend in emission between different systems. There were too much variability [83]. Another study presented emissions for office buildings and residential buildings being at 503 and 402 kg $CO_2/m^2$ [84]. A rough estimate of 500 $CO_2/m^2$ will therefore be used in the calculations.

# 9. Price and emission results

## 9.1. Results - Case 1

Figure 46 shows the calculations for $CO_2$ emissions for Case 1. The result for all three production volumes is 20,4 tonnes $CO_2$/tonne aluminium.

| | | 25 tonnes | 20000 tonnes | 100000 tonnes |
|---|---|---|---|---|
| Production | 20,0 g $CO_2$/g aluminium | | | |
| Truck | 62,0 g $CO_2$/tonne-km | | | |
| Ship | 13,5 g $CO_2$/tonne-km | | | |
| Production - China | | 500 tonnes $CO_2$ | 400000 tonnes $CO_2$ | 2000000 tonnes $CO_2$ |
| Shanghai - Amsterdam | 19455 km | 6,6 tonnes $CO_2$ | 5252,9 tonnes $CO_2$ | 26264,3 tonnes $CO_2$ |
| Amsterdam - Harderwijk | 73,7 km | 0,1 tonnes $CO_2$ | 91,4 tonnes $CO_2$ | 456,9 tonnes $CO_2$ |
| Harderwijk - Amsterdam | 73,7 km | 0,1 tonnes $CO_2$ | 91,4 tonnes $CO_2$ | 456,9 tonnes $CO_2$ |
| Amsterdam - Nörrkoping | 1668 km | 0,6 tonnes $CO_2$ | 450,4 tonnes $CO_2$ | 2251,8 tonnes $CO_2$ |
| Nörrkoping - Finspång | 32 km | 0,05 tonnes $CO_2$ | 39,7 tonnes $CO_2$ | 198,4 tonnes $CO_2$ |
| Finspång - Stavanger | 874 km | 1,4 tonnes $CO_2$ | 1083,8 tonnes $CO_2$ | 5418,8 tonnes $CO_2$ |
| Total | 22176,4 km | 508,8 tonnes $CO_2$ | 407009,4 tonnes $CO_2$ | 2035047,1 tonnes $CO_2$ |
| Tonnes $CO_2$/Mt aluminium | | 20,4 t $CO_2$/Mt alu | 20,4 t $CO_2$/Mt alu | 20,4 t $CO_2$/Mt alu |

**Figure 46:** Case 1 - Emission calculation

Figure 47 shows the calculations for the shipping and production of primary aluminium for Case 1. The result for all three production volumes is 33 910 NOK/tonne aluminium.

| | | 25 tonnes | | 20000 tonnes | | 100000 tonnes | |
|---|---|---|---|---|---|---|---|
| Production | 31800 NOK/tonne | | | | | | |
| Truck | 1,00 NOK/tonne-km | | | | | | |
| Ship | 0,05 NOK/tonne-km | | | | | | |
| Production - China | | 795000 | NOK | 636000000 | NOK | 3180000000 | NOK |
| Shanghai - Amsterdam | 19455 km | 24319 | NOK | 19455000 | NOK | 97275000 | NOK |
| Amsterdam - Harderwijk | 73,7 km | 1843 | NOK | 1474000 | NOK | 7370000 | NOK |
| Harderwijk - Amsterdam | 73,7 km | 1843 | NOK | 1474000 | NOK | 7370000 | NOK |
| Amsterdam - Nörrkoping | 1668 km | 2085 | NOK | 1668000 | NOK | 8340000 | NOK |
| Nörrkoping - Finspång | 32 km | 800 | NOK | 640000 | NOK | 3200000 | NOK |
| Finspång - Stavanger | 874 km | 21850 | NOK | 17480000 | NOK | 87400000 | NOK |
| Total | 22176,4 km | 847739 | NOK | 678191000 | NOK | 3390955000 | NOK |
| NOK/Mt aluminium | | 33910 | NOK/Mt alu | 33910 | NOK/Mt alu | 33910 | NOK/Mt alu |

**Figure 47:** Case 1 - Cost calculation

## 9.2. Results - Case 2

Figure 48 shows the calculations for $CO_2$ emissions for Case 2. The result for all three production volumes is 7,5 tonnes $CO_2$/tonne aluminium.

| | | | 25 tonnes | 20000 tonnes | 100000 tonnes |
|---|---|---|---|---|---|
| Production | 6,7 g CO₂/g aluminium | | | | |
| Truck | 62,0 g CO₂/tonne-km | | | | |
| Ship | 13,5 g CO₂/tonne-km | | | | |
| Import - bauxite | 11279 km | | 15,2 tonnes CO₂ | 12181,3 tonnes CO₂ | 60906,6 tonnes CO₂ |
| Production - Slovenia | | | 167,5 tonnes CO₂ | 134000 tonnes CO₂ | 670000 tonnes CO₂ |
| Talum - Koper | 232 km | | 0,4 tonnes CO₂ | 287,7 tonnes CO₂ | 1438,4 tonnes CO₂ |
| Koper - Nörrkoping | 7305 km | | 2,5 tonnes CO₂ | 1972,4 tonnes CO₂ | 9861,8 tonnes CO₂ |
| Nörrkoping - Finspång | 32 km | | 0,05 tonnes CO₂ | 39,7 tonnes CO₂ | 198,4 tonnes CO₂ |
| Finspång - Stavanger | 874 km | | 1,4 tonnes CO₂ | 1083,8 tonnes CO₂ | 5418,8 tonnes CO₂ |
| Total | 19722 km | | 187,0 tonnes CO₂ | 149564,8 tonnes CO₂ | 747824,0 tonnes CO₂ |
| Tonnes CO₂/Mt aluminium | | | 7,5 t CO₂/Mt alu | 7,5 t CO₂/Mt alu | 7,5 t CO₂/Mt alu |

**Figure 48:** Case 2 - Emission calculation

Figure 49 shows the calculations for the shipping and production of primary aluminium for Case 2. The result for all three production volumes is 35 559 NOK/tonne aluminium.

| | | 25 tonnes | | 20000 tonnes | | 100000 tonnes | |
|---|---|---|---|---|---|---|---|
| Production | 31800 NOK/tonne | | | | | | |
| Truck | 1,00 NOK/tonne-km | | | | | | |
| Ship | 0,05 NOK/tonne-km | | | | | | |
| Import - bauxite | 11279 km | 56395 | NOK | 45116000 | NOK | 225580000 | NOK |
| Production - Slovenia | | 795000 | NOK | 636000000 | NOK | 3180000000 | NOK |
| Talum - Koper | 232 km | 5800 | NOK | 4640000 | NOK | 23200000 | NOK |
| Koper - Nörrkoping | 7305 km | 9131 | NOK | 7305000 | NOK | 36525000 | NOK |
| Nörrkoping - Finspång | 32 km | 800 | NOK | 640000 | NOK | 3200000 | NOK |
| Finspång - Stavanger | 874 km | 21850 | NOK | 17480000 | NOK | 87400000 | NOK |
| Total | 19722 km | 888976 | NOK | 711181000 | NOK | 3555905000 | NOK |
| NOK/Mt aluminium | | 35559 | NOK/Mt alu | 35559 | NOK/Mt alu | 35559 | NOK/Mt alu |

**Figure 49:** Case 2 - Cost calculation

## 9.3. Results - Case 3

Figure 50 shows the calculations for $CO_2$ emissions for Case 3. The amount of tonnes $CO_2$/tonne aluminium is reduced with increasing production volume.

| | | 25 tonnes | 20000 tonnes | 100000 tonnes |
|---|---|---|---|---|
| Building | 500 kg $CO_2$/m$^2$ | | | |
| Production | 2,3 g $CO_2$/g aluminium | | | |
| Truck | 62,0 g $CO_2$/tonne-km | | | |
| Building | 17000 m$^2$ | 8500 tonnes $CO_2$ | 8500 tonnes $CO_2$ | 8500 tonnes $CO_2$ |
| Post consumer | | 57,5 tonnes $CO_2$ | 46000 tonnes $CO_2$ | 230000 tonnes $CO_2$ |
| Bergen - Stavanger | 208 km | 0,1 tonnes $CO_2$ | 51,6 tonnes $CO_2$ | 257,9 tonnes $CO_2$ |
| Fredrikstad - Stavanger | 515 km | 0,2 tonnes $CO_2$ | 127,7 tonnes $CO_2$ | 638,6 tonnes $CO_2$ |
| Oslo - Stavanger | 548 km | 0,2 tonnes $CO_2$ | 135,9 tonnes $CO_2$ | 679,5 tonnes $CO_2$ |
| Tromsø - Stavanger | 2286 km | 0,7 tonnes $CO_2$ | 566,9 tonnes $CO_2$ | 2834,6 tonnes $CO_2$ |
| Trondheim - Stavanger | 1038 km | 0,3 tonnes $CO_2$ | 257,4 tonnes $CO_2$ | 1287,1 tonnes $CO_2$ |
| Total | 4595 km | 8558,9 tonnes $CO_2$ | 55639,6 tonnes $CO_2$ | 244197,8 tonnes $CO_2$ |
| Tonnes $CO_2$/Mt aluminium | | 342,4 t $CO_2$/Mt alu | 2,8 t $CO_2$/Mt alu | 2,4 t $CO_2$/Mt alu |

**Figure 50:** Case 3 - Emission calculation

Figure 51 shows the calculations for the shipping and production of primary aluminium for Case 3. The NOK/tonne aluminium is reduced with increasing production volume.

| | | 25 tonnes | | 20000 tonnes | | 100000 tonnes | |
|---|---|---|---|---|---|---|---|
| Building | 10500 NOK/m$^2$ | | | | | | |
| Production | 19080 NOK/tonne | | | | | | |
| Truck | 5,00 NOK/tonne-km | | | | | | |
| Building | 17000 m$^2$ | 178500000 | NOK | 178500000 | NOK | 178500000 | NOK |
| Post consumer | | 477000 | NOK | 381600000 | NOK | 1908000000 | NOK |
| Bergen - Stavanger | 208 km | 5200 | NOK | 4160000 | NOK | 20800000 | NOK |
| Fredrikstad - Stavanger | 515 km | 12875 | NOK | 10300000 | NOK | 51500000 | NOK |
| Oslo - Stavanger | 548 km | 13700 | NOK | 10960000 | NOK | 54800000 | NOK |
| Tromsø - Stavanger | 2286 km | 57150 | NOK | 45720000 | NOK | 228600000 | NOK |
| Trondheim - Stavanger | 1038 km | 25950 | NOK | 20760000 | NOK | 103800000 | NOK |
| Total | 4595 km | 179091875 | NOK | 652000000 | NOK | 2546000000 | NOK |
| NOK/Mt aluminium | | 7163675 | NOK/Mt alu | 32600 | NOK/Mt alu | 25460 | NOK/Mt alu |

**Figure 51:** Case 3 - Cost calculation

# 10. Discussion - manufacturing value chains

The second objective of the master thesis is to compare different manufacturing value chains for the design alternatives in terms of cost and energy emissions. Three different cases are evaluated, each representing a different production scenario.

Table 4 presents a comparison of the carbon footprints per tonne aluminium produced for the three different cases across the three production volumes. In terms of $CO_2$ emissions per tonne of aluminium, Case 1 consistently shows a carbon footprint of 20,4 tonnes for all production volumes. This high emission level is attributed to the use of coal as an energy source during the production of primary aluminium in China. Case 2, on the other hand, shows significantly lower emissions, with a carbon footprint of 7,5 tonnes per tonne aluminium for all production volumes. This is due to the utilization of nuclear power in Slovenia for primary aluminium production. Interestingly, Case 3, which involves remelting post-consumer aluminium in Norway, exhibits a much higher carbon footprint of 342,4 tonnes $CO_2$ per tonne aluminium for a production volume of 25 tonnes. However, as the production volume increases to 20 000 tonnes and 100 000 tonnes, the carbon footprint decreases significantly to 2,8 tonnes and 2,4 tonnes respectively. The high initial emissions are due to the construction of the factory. This results in high emissions per tonne aluminium produced for low production volumes. And the emission will decrease for increasing production volumes, approaching the emission rate for post-consumer aluminium.

**Table 4:** Comparison of carbon footprint

| t $CO_2$/Mt aluminium | | | |
|---|---|---|---|
| Production volume | **25 Mt** | **20 000 Mt** | **100 000 Mt** |
| Case 1 | 20,4 | 20,4 | 20,4 |
| Case 2 | 7,5 | 7,5 | 7,5 |
| Case 3 | 342,4 | 2,8 | 2,4 |

Table 5 presents a comparison of the price in NOK per tonne aluminium produced for the three different cases across the three production volumes. Case 1 and Case 2, are assumed to have equal aluminium prices. They have relatively similar cost per tonne aluminium, with Case 1 slightly better. Despite Case 1 having a longer transportation length, the shipping cost for Case 2 is twice as high. This is due to the fact that the cost rate takes into account the load, which is four times greater for the importation of bauxite from Brazil. This could show a weakness in the cost rate used in the shipping calculation. In terms of production cost, Case 3 using post-consumer scrap is the most expensive option for low production volume. However, it becomes the least expensive for larger volumes. This is mainly due to the high investment cost associated with construction of a new factory. The high initial investment means that the price per tonne of aluminium is high for small volumes and will decrease as the volumes is increased.

**Table 5:** Comparison of price

| NOK/t aluminium | | | |
|---|---|---|---|
| Production volume | **25 t** | **20 000 t** | **100 000 t** |
| Case 1 | 33 910 | 33 910 | 33 910 |
| Case 2 | 35 559 | 35 559 | 35 559 |
| Case 3 | 7 163 675 | 32 600 | 25 460 |

Case 3 is the most expensive case when it comes to shipping. Once again, this is likely a weakness in the cost rate. It would be reasonable to assume that a case involving transportation within the country by truck would be less expensive than shipping aluminium across the world. For Case 3, it could be beneficial with a couple of detours to combine some of the routes as long as the truck is not fully loaded. Combining Tromsø/Trondheim as well as Fredrikstad/Oslo would reduce the total distance of 1 582 km.

It is important to acknowledge that the numbers and results should be interpreted with caution. The difficulty in obtaining precise values due to agreed prices, confidentiality, and the need for assumptions and calculations based on limited information may introduce uncertainties. Further research and data collection are recommended to refine the results and reduce uncertainties. Collaborations with industry partners and access to detailed cost and emission data would improve the accuracy and reliability of the findings. Additionally, the consideration of carbon tax as an important factor in a real-life situation is recognized but overlooked to simplify the calculations in the thesis. An other important factor in the production lines is time. Some companies may have tight deadlines, where there is no room for delays. Longer transport, more time-consuming transport methods and more intermediate stops will result in longer delivery time, which could be crucial.

The comparison of the different manufacturing value chains provides insights into the cost and energy emission implications of each scenario. The findings suggest that production volume is an important factor with regard to which production structure is favorable. Case 3 is the least favorable choice for both cost and emission per tonne aluminium produced for low production volumes, due to the construction. With increasing production volumes, these numbers decrease, making it the most favorable option for large production volumes. The manufacturing process for recycled aluminium requires less heat and energy, resulting in reduced emissions that contribute to $CO_2$ levels in the environment. And with the ever-increasing focus on minimizing emissions, using post-consumer aluminium is the future. The quantifying of the value of premium aluminium is however still a challenge. Having to construct a factory will result in large investment for both cost and emission in the construction phase. Thus, the situation would turn into a matter of evaluation, considering both the financial and environmental benefits for large production volumes. An investment for less cost and emissions in the years to come could be beneficial.

# 11. Conclusion and further work

This master thesis is aimed to address two interconnected aspects: joining methods for offshore wind turbine components and the evaluation of different manufacturing value chains for the design alternatives. By examining both areas, a comprehensive understanding can be gained to inform decision-making and contribute to the development of efficient and sustainable offshore wind turbines.

The discussion on joining methods encompassed three techniques: MIG welding, bolt connection, and extruded T-track with bolt connection. Each method was assessed based on strength, material use, complexity, and manufacturability. MIG welding demonstrated high strength with low material, moderate complexity and low manufacturability. Bolt connection offered moderate strength, low material use, low complexity and high manufacturablity. The extruded T-track with bolt connection showed high strength, high material use, moderate complexity and moderate manufacturability. It is important to note that the calculations and simulations considered static loads, while dynamic loads and fatigue life should be considered for a comprehensive evaluation. This is necessary to create a joint applicable for prototyping.

In evaluating the manufacturing value chains, three cases were analysed: primary aluminium production in China using coal, primary aluminium production in Slovenia using nuclear energy, and gathering post-consumer metal in Norway for remelting. For the three cases, three different production volumes were analysed: 25, 20 000 and 100 000 tonnes. The assessment focused on cost and energy emissions. The results revealed that Case 1 and Case 2 were not affected by production volume. However, Case 3 exhibited significant variations in carbon footprints across different production volumes. The construction of the factory resulted in high initial cost and emissions, making it the least favorable option for low production volumes. For larger volumes, the values decreased, making it the most favorable option. The utilization of post-consumer scrap presents an excellent opportunity to decrease emissions, aligning well with the growing emphasis on sustainability. The integrated production line could be beneficial for the future, but needs to be carefully considered due to the high investment in terms of cost and emissions. It is important to acknowledge that data availability and accuracy posed challenges, and further research and collaboration with industry partners are recommended to refine the results.

The integration of these discussions highlights the importance of considering both the joining methods and manufacturing value chains in the development of offshore wind turbines. Selecting appropriate joining methods is crucial for ensuring structural integrity, optimizing material usage, and achieving efficient manufacturability. Simultaneously, evaluating the manufacturing value chains enables the identification of cost-effective and environmentally responsible approaches. By combining these considerations, it becomes possible to design offshore wind turbines that are not only structurally robust but also manufactured using sustainable practices.

The research provides valuable insights but also highlights the need for additional research, collaboration, and access to detailed data to enhance the reliability of the findings. Continued efforts in refining the understanding of joining methods, exploring alternative manufacturing value chains, and addressing dynamic loads and fatigue life. This will contribute to the ongoing development and growth of the renewable energy sector.

In conclusion, this thesis contributes to the knowledge and understanding of joining methods and manufacturing value chains for offshore wind turbines. By incorporating these insights into the decision-making process, it is possible to develop turbines that are both technologically advanced and environmentally sustainable, supporting the transition to a cleaner and more efficient energy future.

# References

[1] National Geographic: *Renewable energy, explained.* https://www.nationalgeographic.com/environment/article/renewable-energy, visited on 2023-05-04.

[2] Stortinget: *Eu-strategi for vindkraft til havs.* https://www.stortinget.no/no/Hva-skjer-pa-Stortinget/EU-EOS-informasjon/EU-EOS-nytt/2020/eueos-nytt---26.-november-2020/eu-strategi-for-vindkraft-til-havs/, visited on 2023-02-01.

[3] Hydro: *Facts about aluminium.* https://www.hydro.com/en/aluminium/about-aluminium/facts-about-aluminium/, visited on 2023-02-08.

[4] Elverum, Christer W.: *Agile product development and set-based design.* Lecture, September 2022. Access limited to registered course participants.

[5] Smartsheet: *The power of iterative design and process.* https://www.smartsheet.com/iterative-process-guide, visited on 2023-05-30.

[6] Dassault Systemes: *Abaqus/cae.* https://www.3ds.com/products-services/simulia/products/abaqus/abaquscae/, visited on 2023-05-04.

[7] Dassault Systemes: *Abaqus/cae cad interfaces.* https://www.3ds.com/products-services/simulia/products/abaqus/add-ons/cad-associative-interfaces/, visited on 2023-05-04.

[8] Dassault Systemes: *Solidworks.* https://www.3ds.com/products/solidworks, visited on 2023-05-04.

[9] National Geographic: *Wind energy.* https://education.nationalgeographic.org/resource/wind-energy/, visited on 2023-02-01.

[10] Office of ENERGY EFFICIENCY and RENEWABLE ENERGY: *Top 10 things you didn't know about offshore wind energy.* https://www.energy.gov/eere/wind/articles/top-10-things-you-didnt-know-about-offshore-wind-energy, visited on 2023-02-02.

[11] Orsted: *1991-2001, the first offshore wind farms.* https://orsted.com/en/insights/white-papers/making-green-energy-affordable/1991-to-2001-the-first-offshore-wind-farms, visited on 2023-05-05.

[12] Reve: *Hornsea 2, the world's largest wind farm, enters full operation.* https://www.evwind.es/2022/08/31/hornsea-2-the-worlds-largest-wind-farm-enters-full-operation/87630, visited on 2023-05-05.

[13] American Geosciences Institute: *What are the advantages and disadvantages of offshore wind farms?* https://www.americangeosciences.org/critical-issues/faq/what-are-advantages-and-disadvantages-offshore-wind-farms, visited on 2023-02-01.

[14] Mouser Electronics: *Wind turbines: Tiny sensors play big role.* https://eu.mouser.com/applications/tiny-Sensors-Role-in-Wind-Turbines/, visited on 2023-04-03.

[15] Britannica: *Wind turbine.* https://www.britannica.com/technology/wind-turbine, visited on 2023-01-16.

[16] National Geographic: *Anemometer.* https://education.nationalgeographic.org/resource/anemometer, visited on 2023-01-26.

[17] Office of ENERGY EFFICIENCY and RENEWABLE ENERGY: *How a wind turbine works - text version.* https://www.energy.gov/eere/wind/how-wind-turbine-works-text-version, visited on 2023-01-27.

[18] Fazal, Muhammad Rayyan and Kamran, Muhammad: *Renewable Energy Conversion Systems.* Academic Press, 2021.

[19] Kim, Manuel and Dalhoff, Peter: *Yaw systems for wind turbines ? overview of concepts, current challenges and design methods.* Journal of Physics: Conference Series, 524:12–86, June 2014.

[20] Beig, Abdul R. and Muyeen, S.M.: *Electric Renewable Energy Systems.* Academic Press, 2016.

[21] JIAYAO CO., LMT: *Difference between a tubular tower and an angular tower.* https://www.telecommunicationtower.com/news/compare-tubular-towers-and-angular-towers-36.html, visited on 2023-05-17.

[22] Office of Energy Efficiency & Renewable Energy: *How does a wind turbine work?* https://www.energy.gov/eere/how-does-wind-turbine-work, visited on 2023-05-05.

[23] ResearchGate: *Constructing a plastic bottle wind turbine as a practical aid for learning about using wind energy to generate electricity.* https://www.researchgate.net/figure/Schematic-view-of-the-operation-of-a-wind-turbine_fig3_231060194, visited on 2023-05-05.

[24] Energy Education: *Betz limit.* https://energyeducation.ca/encyclopedia/Betz_limit, visited on 2023-05-05.

[25] USGS: *What materials are used to make wind turbines?* https://www.usgs.gov/faqs/what-materials-are-used-make-wind-turbines, visited on 2023-04-20.

[26] Semprius: *What are wind turbine blades made of?* https://www.semprius.com/what-are-wind-turbine-blades-made-of/, visited on 2023-01-16.

[27] Bloomberg: *Wind turbine blades can't be recycled, so they're piling up in landfills.* https://www.bloomberg.com/news/features/2020-02-05/wind-turbine-blades-can-t-be-recycled-so-they-re-piling-up-in-landfills, visited on 2023-02-06.

[28] World Wide Wind: *Next generation floating offshore wind.* https://worldwidewind.no, visited on 2023-03-01.

[29] Bernhoff, Hans and Mikkelsen, Kolbjørn: *Offshore wind turbine design.* 2023-05-25 [World Wide Wind]. Location: Digital meeting/mail.

[30] Collins, Danielle: *Rotary bearings: Summary of types and variations.* https://www.motioncontroltips.com/rotary-bearings-types-and-variations/, visited on 2023-03-08.

[31] Xin, Qianfan: *Durability and reliability in diesel engine system design.* Diesel Engine System Design, pages 113–202, 2013.

[32] Garrafa-Pacheco, Leonardo F. and Miramontes, Orlando: *Time series rainflow analysis for fatigue life calculation*, November 2021. https://www.researchgate.net/publication/356665059_Time_Series_Rainflow_Analysis_For_Fatigue_Life_Calculation, visited on 2023-06-05.

[33] Halmøy, Einar: *Sveiseteknikk.* Akademika, 2017.

[34] Sensharma, Pradeep and Collette, Matthew and Harrington, Joey: *Effect of welded properties on aluminum structures.* http://www.shipstructure.org/proj/yabbfiles/Attachments/SR_1460_Final_Report.pdf, visited on 2023-03-07.

[35] Benson, Simon and Downes, Jon and Dow, R.S: *Ultimate strength characteristics of aluminium plates for high-speed vessels.* Ships and Offshore Structures, 6:67–80, March 2011.

[36] Du Toit, Madeleine and Mutombo, Kalenda: *The influence of pulsed gas metal arc welding on the fatigue and corrosion-fatigue properties of wrought aluminium 6061-t651.* Anti-Corrosion Methods and Materials, 66:719–729, August 2019.

[37] European Committee for Standardization (CEN): *NS-EN 1999-1-1:2007+A1:2009+NA:2009.* Technical report, Norwegian Standards (NS), 2017.

[38] Myklebost, Per Christian Aas: *Joining calculation.* 2023-05-25 [Northwest Solutions AS]. Location: Digital meeting/mail.

[39] Hydal: *Aluminium profiler.* https://hap.hydal.com/download-file.php?file_id=1661&temp_id=71880976, visited on 2023-03-12.

[40] Lin, Weiwei and Yoda, Teruhiko: *Steel bridges.* Bridge Engineering, pages 111–136, 2017.

[41] Soetens, F.: *Design of connections.* No year available.

[42] EurocodeApplied.com: *Table of design properties for metric steel bolts m5 to m39 - eurocode 3.* https://eurocodeapplied.com/design/en1993/bolt-design-properties, visited on 2023-06-04.

[43] fasteners, Orbital: *M10 x 200 high tensile hex bolt grade 8.8 galvanised, din 931 - orbital fasteners.* https://www.orbitalfasteners.co.uk/products/m10-x-200-high-tensile-hex-bolt-grade-8-8-galvanised-din-931, visited on 2023-06-04.

[44] Momentum Manufacturing Group - Engineered Extrusions: *Aluminum extrusion manufacturing 101: Understanding extrusion die types.* https://mmgextrusions.com/resources/aluminum-extrusion-die-types/, visited on 2023-04-12.

[45] Aluminium Extruders Council: *Aluminum extrusion alloys & tempers.* https://aec.org/alloys-tempers, visited on 2023-05-20.

[46] RAESA: *Mechanical properties.* https://www.aluminiumprofilesraesa.com/en/70828/Technical-data/Mechanical-properties.htm, visited on 2023-05-07.

[47] MakeItFrom.com: *6005-t6 aluminum.* https://www.makeitfrom.com/material-properties/6005-T6-Aluminum, visited on 2023-05-07.

[48] Ferguson Perforating: *6061 aluminium alloy.* https://www.fergusonperf.com/the-perforating-process/material-information/specialized-aluminum/6061-aluminium-alloy/, visited on 2023-05-07.

[49] MakeItFrom.com: *6061-t6 aluminum.* https://www.makeitfrom.com/material-properties/6061-T6-Aluminum, visited on 2023-05-07.

[50] The Engineering Toolbox: *Aluminum alloys - mechanical properties.* https://www.engineeringtoolbox.com/properties-aluminum-pipe-d_1340.html, visited on 2023-05-07.

[51] MakeItFrom.com: *6063-t6 aluminum.* https://www.makeitfrom.com/material-properties/6063-T6-Aluminum, visited on 2023-05-07.

[52] YIEH CORPORATION LIMITED: *Technical data sheet (tds).* https://aluminum.yieh.com/Upfiles/EDUp/files/6000%20Series/TDS/AA6082/TDS-YIEH-6082-Plate.pdf, visited on 2023-05-07.

[53] MakeItFrom.com: *6082-t6 aluminum.* https://www.makeitfrom.com/material-properties/6082-T6-Aluminum, visited on 2023-05-07.

[54] Casademunt, Alexandre Morato and Sriramula, Srinivas: *Calibration of safety factors for offshore wind turbine support structures using fully coupled simulations.* Marine Structures, 75:1–14, January 2021.

[55] 4RealSim: *Mesh quality checks tools abaqus.* https://www.4realsim.com/mesh-quality-checks-tools-abaqus/, visited on 2023-05-25.

[56] Hydro: *How is aluminium made?* https://www.hydro.com/en-NO/aluminium/about-aluminium/how-its-made/, visited on 2023-06-01.

[57] Scientific Figure on ResearchGate: *The aluminum smelting process and innovative alternative technologies.* https://www.researchgate.net/figure/Flow-sheet-of-the-aluminum-production-process_fig3_262148554, visited on 2023-06-01.

[58] Ecta: *Guidelines for measuring and managing co2 emission from freight transport operations.* https://www.ecta.com/wp-content/uploads/2021/03/ECTA-CEFIC-GUIDELINE-FOR-MEASURING-AND-MANAGING-CO2-ISSUE-1.pdf, visited on 2023-03-08.

[59] European Commission: *2030 climate target plan.* https://climate.ec.europa.eu/eu-action/european-green-deal/2030-climate-target-plan_en, visited on 2023-03-08.

[60] Osborne, Jorunn Fjeld: *Shipping solution for Hydro.* 2023-05-26 [Hydro]. Location: Digital meeting.

[61] ING Think: *Aluminium smelter shutdowns threaten europe's green transition.* https://think.ing.com/articles/aluminium-smelter-shutdowns-threaten-europes-green-transition/, visited on 2023-05-10.

[62] Wicona: *Hydro circal recycled aluminium.* https://www.wicona.com/en/int/sustainability/beyond-materials/hydro-circal-recycled-aluminium/, visited on 2023-05-25.

[63] Furu, Oddgeir: *Aluminium marked.* 2023-04-18 [Hydro]. Location: E-mail.

[64] European Commission: *Carbon border adjustment mechanism.* https://taxation-customs.ec.europa.eu/green-taxation-0/carbon-border-adjustment-mechanism_en, visited on 2023-03-28.

[65] China Dialogue: *How will eu's 'green tariff' impact china's carbon market?* https://chinadialogue.net/en/climate/how-will-eus-green-tariff-impact-chinas-carbon-market/, visited on 2023-03-28.

[66] European Commission: *Eu emissions trading system (eu ets).* https://climate.ec.europa.eu/eu-action/eu-emissions-trading-system-eu-ets_en, visited on 2023-03-28.

[67] NVE: *Nve temakart.* https://temakart.nve.no/tema/havvind, visited on 2023-05-28.

[68] Mining Technology: *Bauxite production in china and major projects.* https://www.mining-technology.com/data-insights/bauxite-in-china/, visited on 2023-06-05.

[69] National Geographic: *Fossil fuels.* https://education.nationalgeographic.org/resource/fossil-fuels/, visited on 2023-05-28.

[70] Statista: *Distribution of electricity generation in china in 2022, by source.* https://www.statista.com/statistics/1235176/china-distribution-of-electricity-production-by-source/, visited on 2023-05-29.

[71] Carboncare: *Co2 emissions calculator.* https://www.carboncare.org/en/co2-emissions-calculator.html, visited on 2023-03-07.

[72] AlCircle: *Slovenia's talum shuts down its primary aluminium production.* https://www.alcircle.com/news/slovenia-s-talum-shuts-down-its-primary-aluminium-production-91157, visited on 2023-03-08.

[73] Talum: *Cds – electric energy.* https://www.talum.si/en/elektrika.html, visited on 2023-05-29.

[74] National Geographic: *Nuclear energy.* https://education.nationalgeographic.org/resource/nuclear-energy/, visited on 2023-05-28.

[75] Volza: *Bauxite imports in slovenia - import data with price, buyer, supplier, hsn code.* https://www.volza.com/p/bauxite/import/import-in-slovenia/, visited on 2023-06-05.

[76] Aluminiumleader: *How aluminium is produced.* https://www.aluminiumleader.com/production/how_aluminium_is_produced/, visited on 2023-06-05.

[77] Energifakta Norge: *Electricity production.* https://energifaktanorge.no/en/norsk-energiforsyning/kraftproduksjon/, visited

on 2023-05-29.

[78] National Geographic: *Hydroelectric energy.* https://education.nationalgeographic.org/resource/hydroelectric-energy/, visited on 2023-05-28.

[79] Hydro: *Hydro circal recycled aluminium.* https://www.hydro.com/en/aluminium/products/low-carbon-and-recycled-aluminium/low-carbon-aluminium/hydro-circal/, visited on 2023-05-25.

[80] Wikimedia Commons: *Norway population density.* https://commons.wikimedia.org/wiki/File:Norway_population_density.gif, visited on 2023-04-25.

[81] Ringen, Geir: *Report on capex for an integrated greenfield plant for fabrication of large scale aluminium modules – a benchmark study.* pages 1–8, April 2021.

[82] Zainordin, Nadzirah and Dhuny, Bibi Fatimah: *Factors contributing to carbon emission in construction activity*, January 2020.

[83] Gervasio, H. and Dimova, S.: *Environmental benchmarks for buildings*, 2018, ISBN 978-92-79-80970-5. JRC110085.

[84] Share Your Green Design: *The embodied carbon of buildings.* https://www.shareyourgreendesign.com/the-embodied-carbon-of-buildings-2/, visited on 2023-06-03.
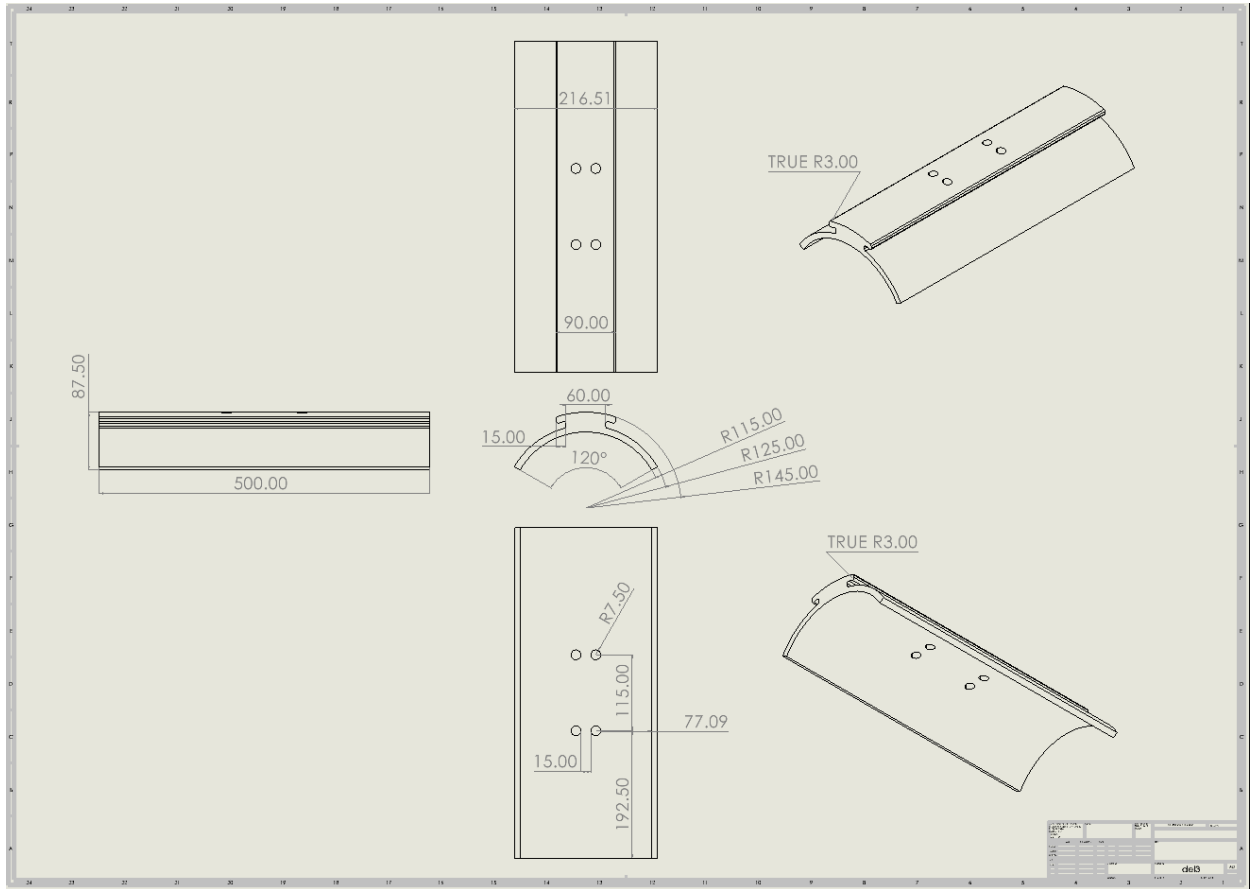
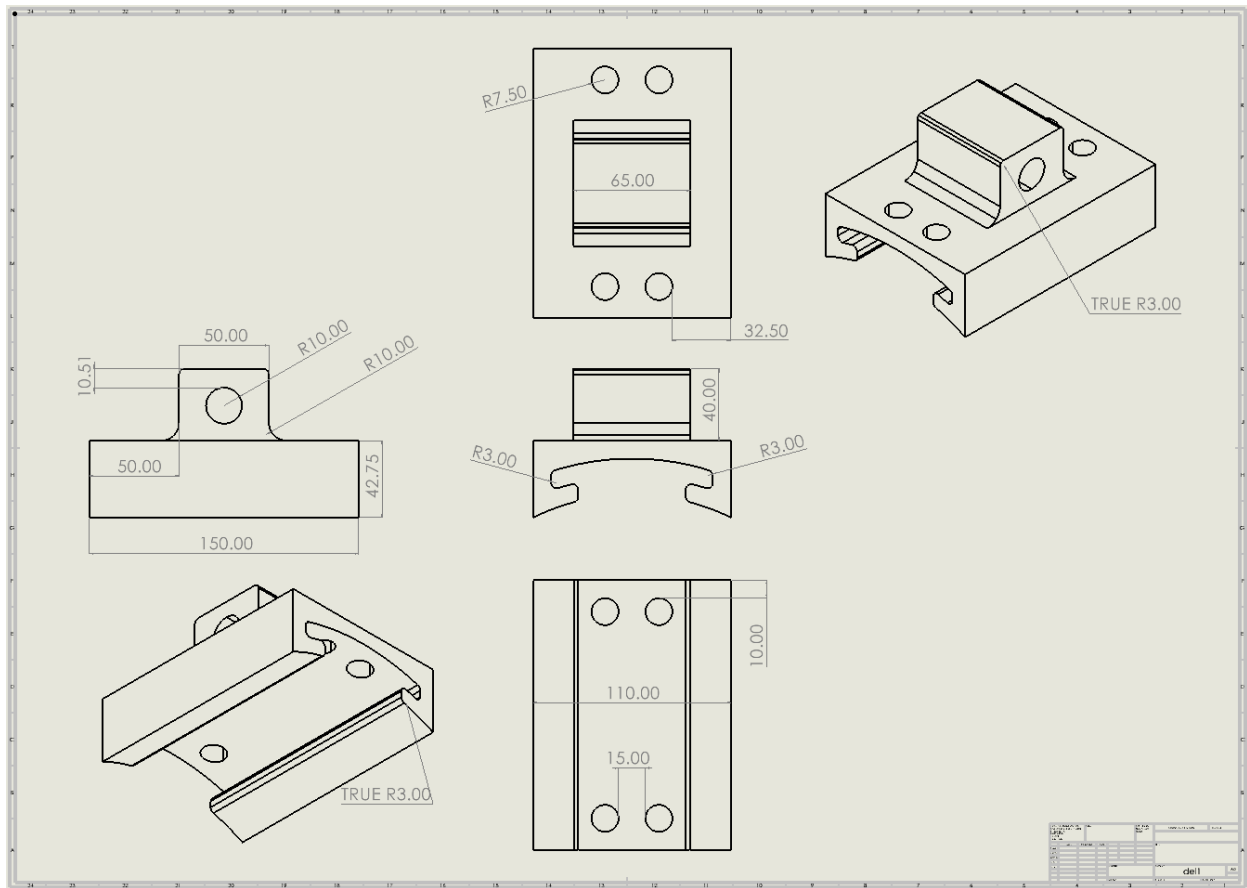# Appendix



**Figure A-1:** Mechanical drawing of mast [1:1,6]

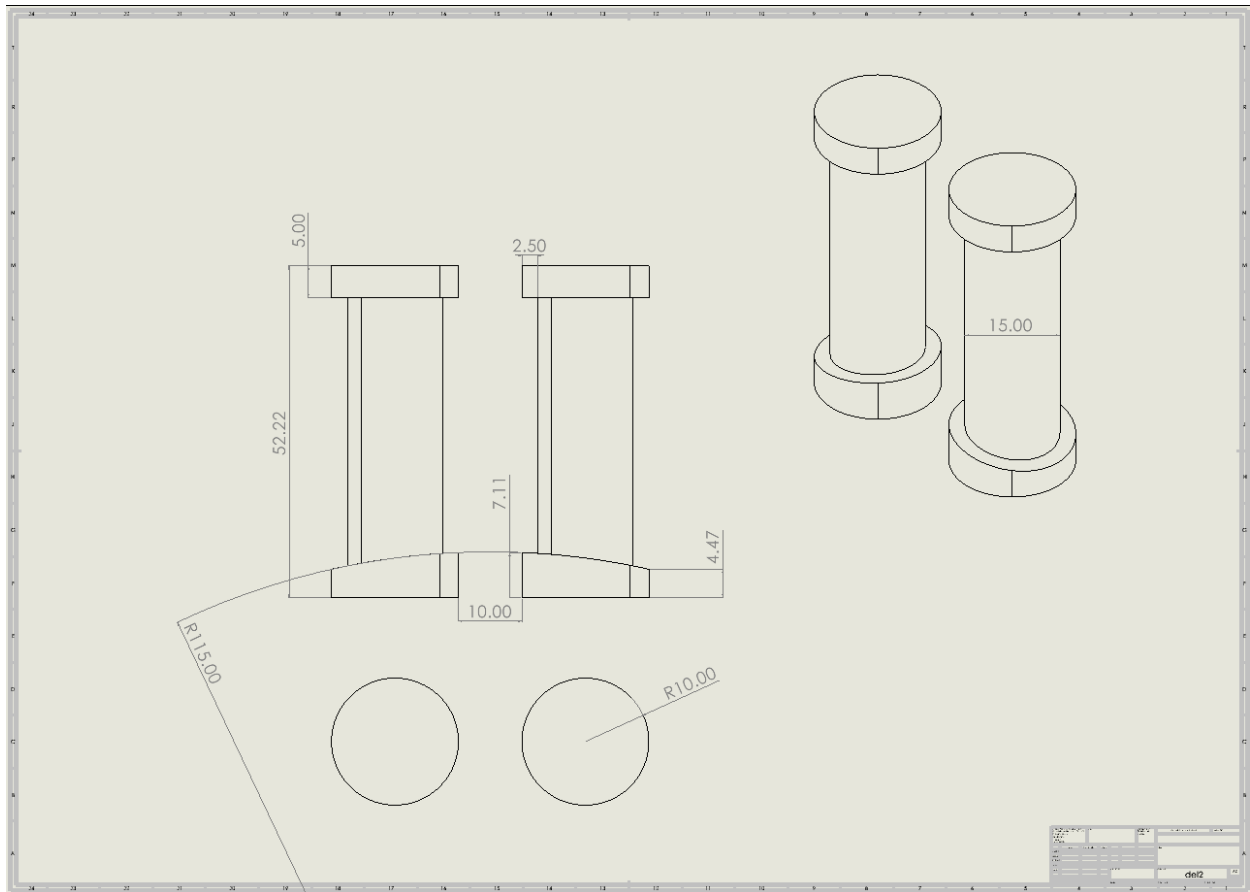**Figure A-2:** Mechanical drawing of bracket [1,7:1]

**Figure A-3:** Mechanical drawing of bolts [6:1]